UNITED NATIONS EDUCATIONAL, SCIENTIFIC AND CULTURAL ORGANIZATION
INTERNATIONAL ATOMIC ENERGY AGENCY
INTERNATIONAL CENTRE FOR THEORETICAL PHYSICS
I.C.T.P., P.O. BOX 586, 34100 TRIESTE, ITALY, CABLE: CENTRATOM TRIESTE

SMR/930 - 30

"Workshop on El Niño, Southern Oscillation and Monsoon"
15 - 26 July 1996

"ENSO-Monsoon Interactions"

R. LUKAS
University of Hawaii
Honolulu
USA

Please note: These are preliminary notes intended for internal distribution only.

ENSO-Monsoon Interactions

Roger Lukas
University of Hawaii

Workshop on El Nino,
Southern Oscillation and Monsoon

International Centre for Theoretical Physics

Trieste, Italy
July 15-26, 1996

Overview

- Multiple time-scale interactions
- Interaction between zonal and meridional circulations
  - Walker and regional Hadley circulations
  - Zonal equatorial flows and western boundary currents
- Convection provides essential nonlinearity

Asian-Australian Monsoon ↔ ENSO

Time Scale	Associated Characteristics	Relation to ENSO
nnual Mean Monsoon	* "land-locked" convection reinforced by warm pool convection * Walker circulation ↔ equatorial thermocline (sea level) slope and SST gradient (Bjerknes) * Mean ocean circulation (tropics; subtropics?) especially westward South Equatorial Current and North Equatorial Current, and Indonesian Throughflow	land-locked convective heating rate ⇒ ENSO period
ean Monsoon cycle	* convection not locked tightly to land – both land + ocean solar heating * Walker circulation + [WPAC] trade wind variation * Annual Kelvin and Rossby waves (remote forcing) * Vertical mixing + Ekman pumping (local forcing)	determines ENSO onset + decay characteristics
terannually-variable Monsoon	* competition for convection between land + ocean * zonal migrations of warm pool and ascending branch of Walker circulation * modulation of annual Rossby wave * western Pacific boundary currents and Indonesian Throughflow responses	interaction with ENSO

Multiple time-scale interactions

- intraseasonal - annual - biennial - quadrennial (ENSO) - decadal
- Low frequency state of coupled ocean-atmosphere-land system determines gross ENSO characteristics
- Annual cycle determines onset and decay characteristics

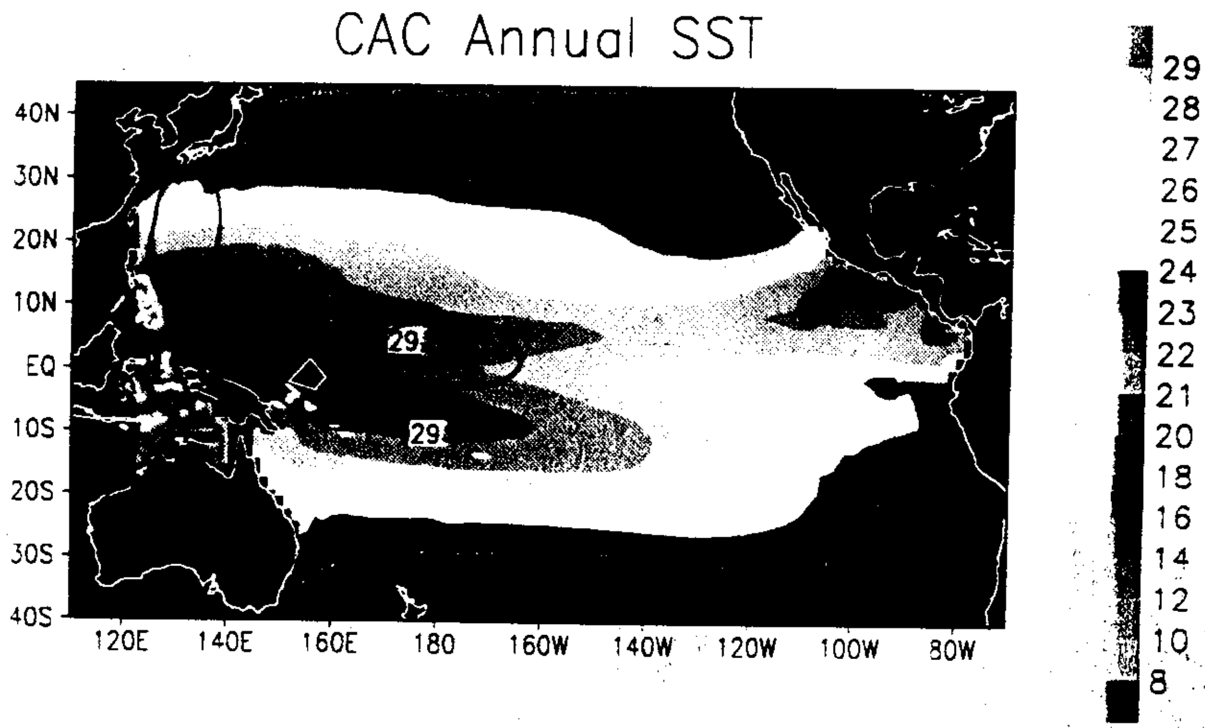
CAC Annual SST
40N
30N
20N
10N
EQ
10S
20S
30S
40S
120E 140E 160E 180 160W 140W 120W 100W 80W
29
29
29 28 27 26 25 24 23 22 21 20 18 16 14 12 10 8

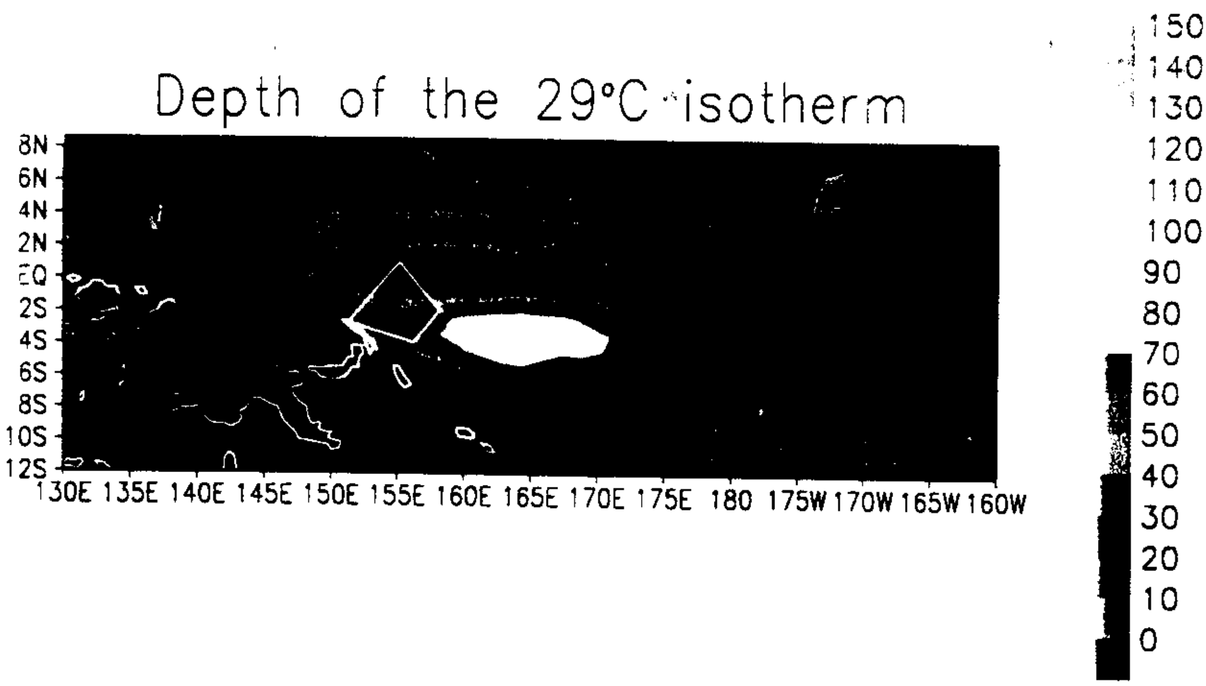
Depth of the 29°C isotherm
8N
6N
4N
2N
EQ
2S
4S
6S
8S
10S
12S
130E 135E 140E 145E 150E 155E 160E 165E 170E 175E 180 175W 170W 165W 160W
150 140 130 120 110 100 90 80 70 60 50 40 30 20 10 0

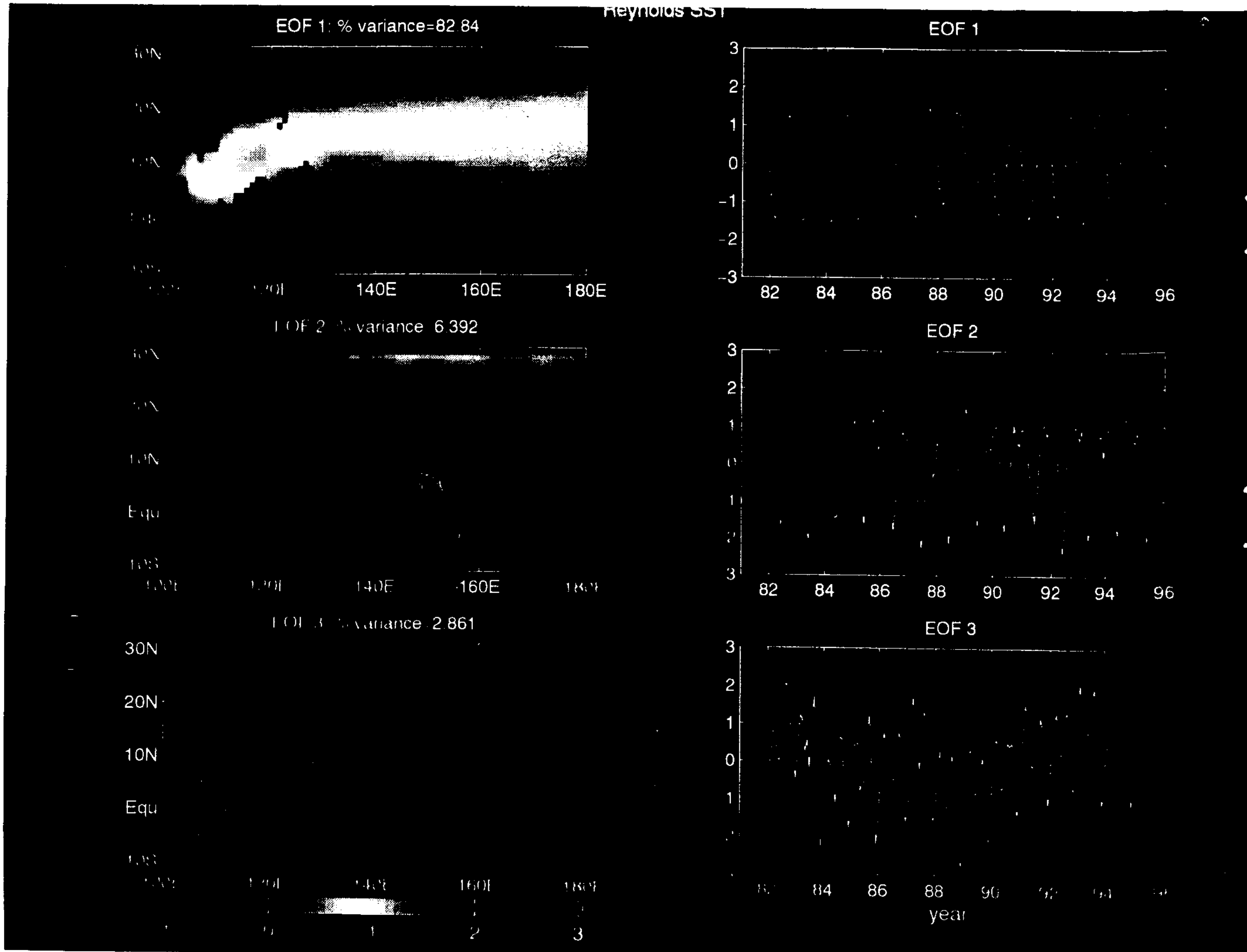
Reynolds SST
EOF 1: % variance=82.84
140E
160E
180E
EOF 2 % variance 6.392
140E
160E
EOF 3 % variance 2.861
30N
20N
10N
Equ
1
2
3
EOF 1
EOF 2
EOF 3
3
2
1
0
-1
-2
-3
82
84
86
88
90
92
94
96
year

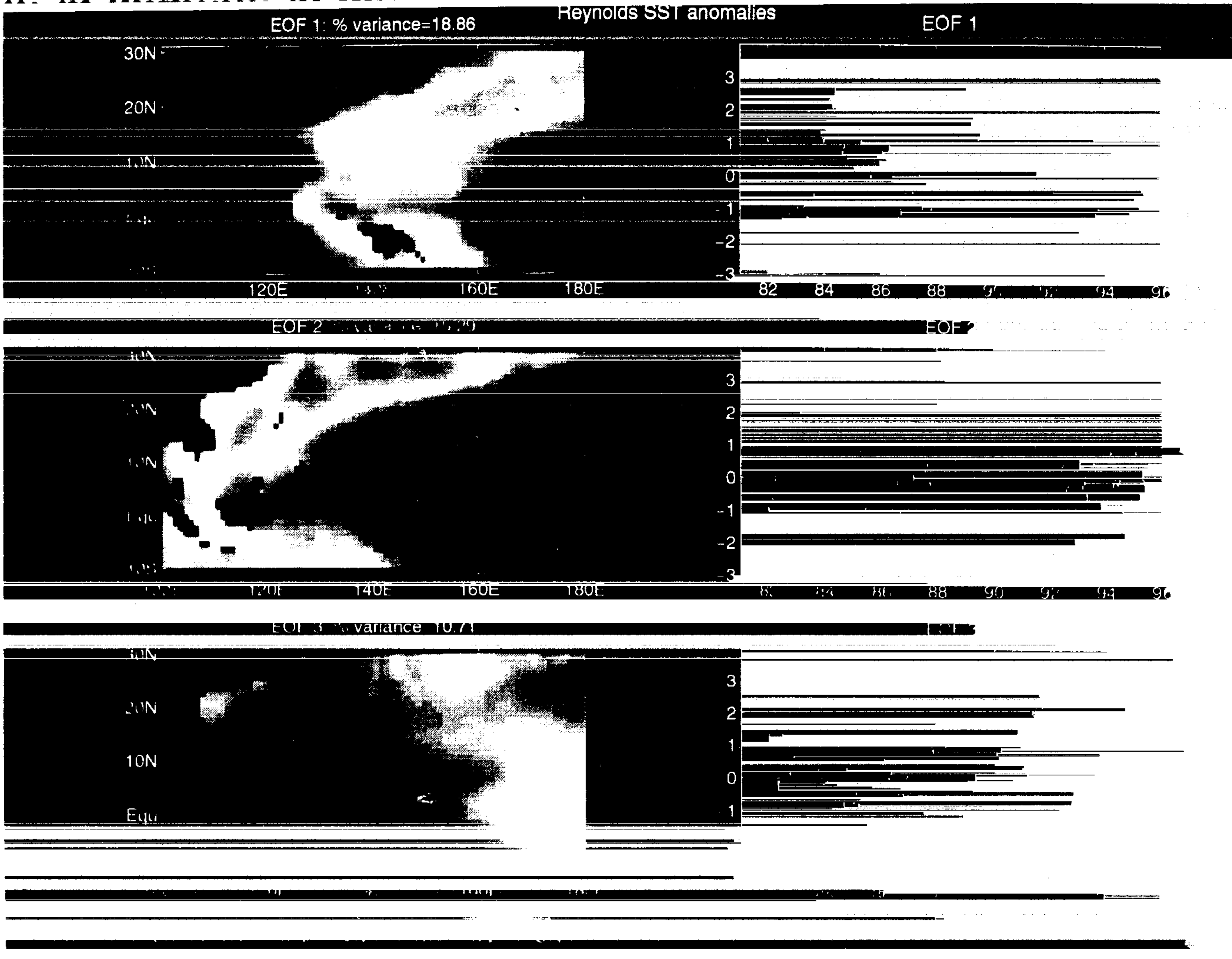

Reynolds SST anomalies
EOF 1: % variance=18.86
EOF 1
30N
20N
120E
160E
180E
82
84
86
88
94
EOF 2
120E
140E
160E
180E
88
90
94
10N
Equ


Pacific W
ing of N. Equato
The Pacific Ocean
Ocean and
Bengal

PACIFIC OCEAN LOW-LATITUDE WESTERN BOUNDARY CURRENTS AND THE INDONESIAN THROUGHFLOW

Mean State of Equatorial Pacific

- Zonal wind stress along the equator
- Thermocline slope along equator
- SST gradient along equator

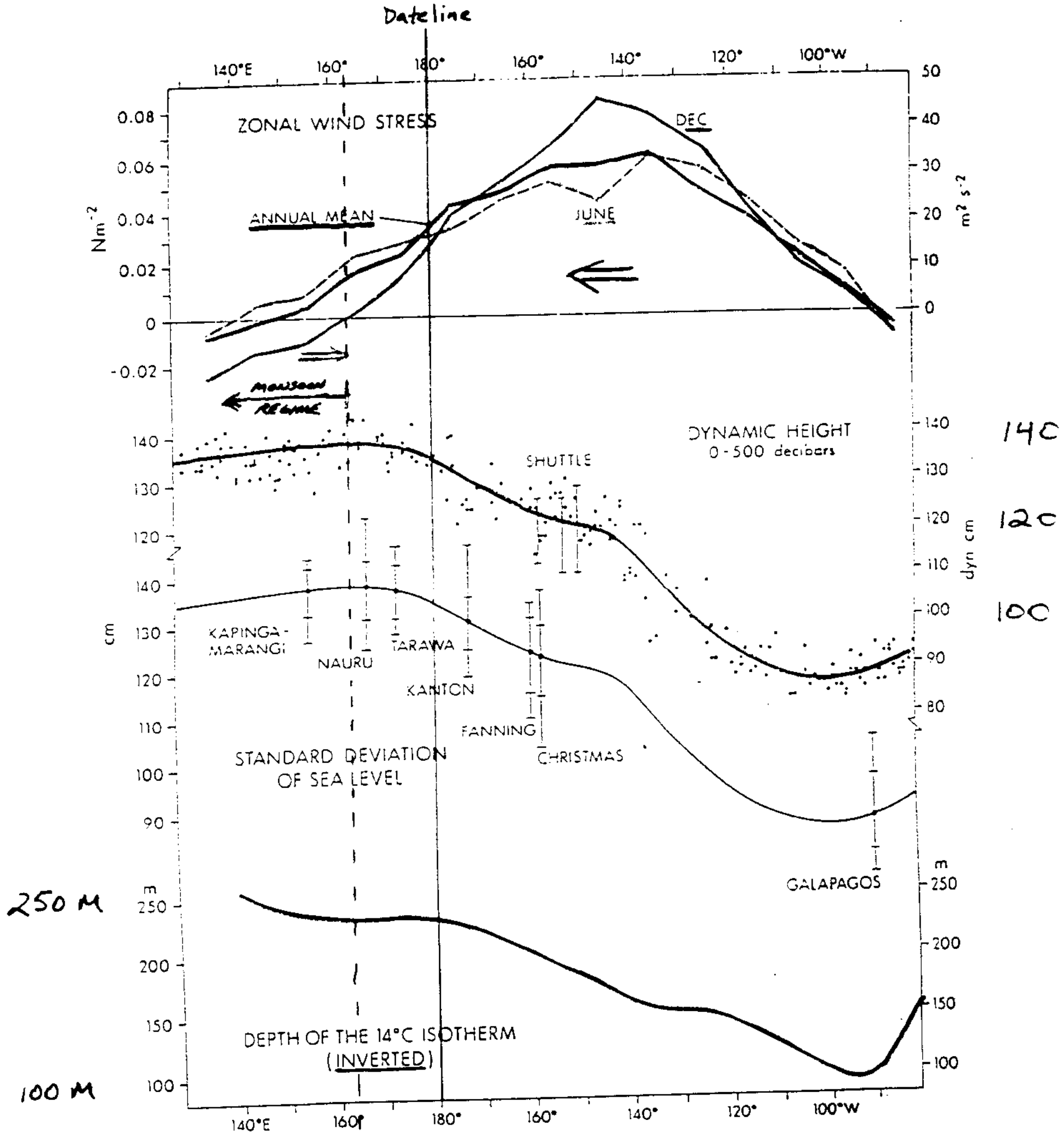

Dateline
140°E
160°
180°
160°
140°
120°
100°W
ZONAL WIND STRESS
DEC
ANNUAL MEAN
JUNE
Nm⁻²
m² s⁻²
MONSOON REGIME
DYNAMIC HEIGHT
0-500 decibars
SHUTTLE
dyn cm
14C
12C
10C
KAPINGA-MARANGI
NAURU
TARAWA
KANTON
FANNING
CHRISTMAS
GALAPAGOS
cm
STANDARD DEVIATION OF SEA LEVEL
250 M
100 M
DEPTH OF THE 14°C ISOTHERM
(INVERTED)

Wyrtki (1984)

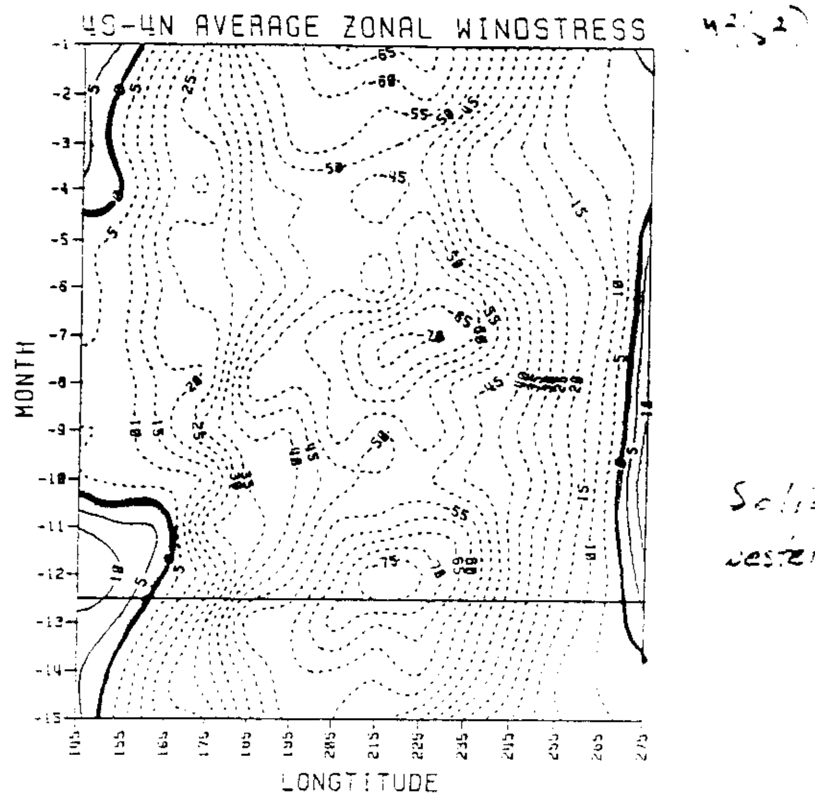

Solid contours are western (eastward)

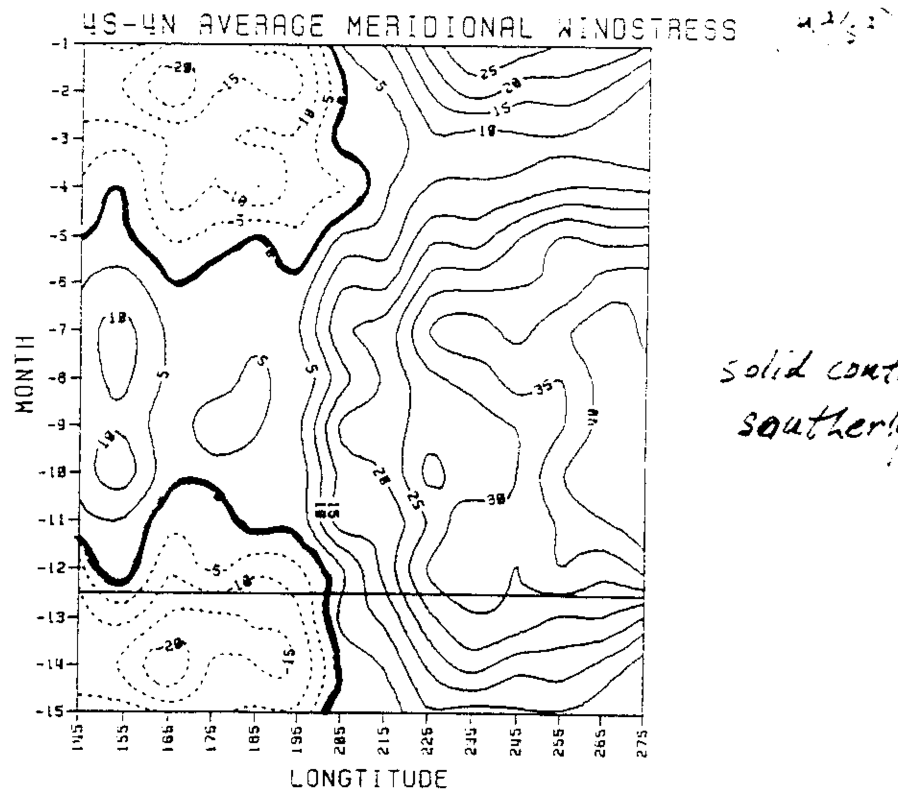

solid contours are southerly (northward)

based on Wyrtki and Meyers
wind stress climatology

$\tau^{x'}$

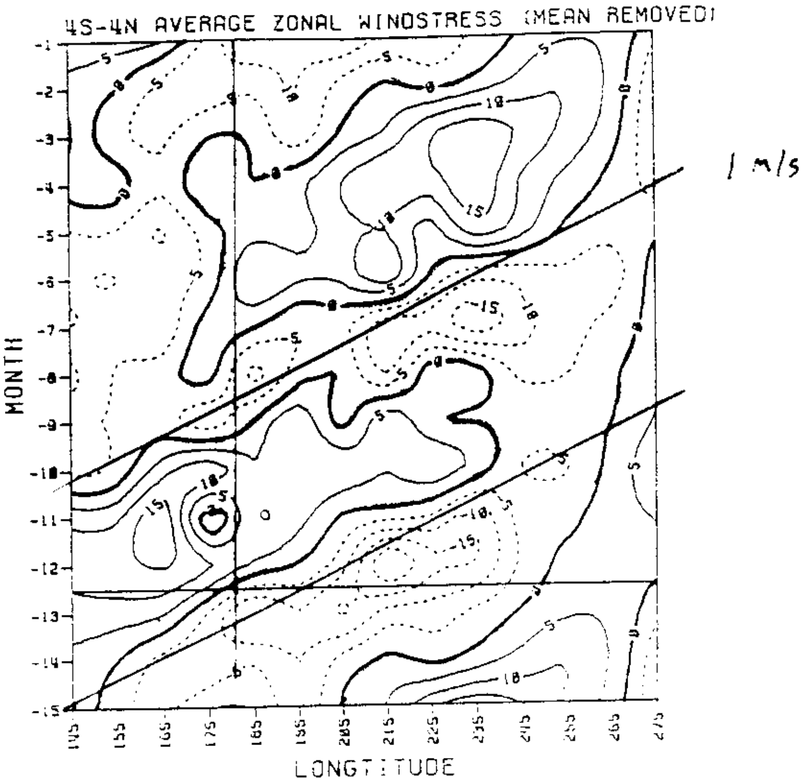

4S-4N AVERAGE ZONAL WINDSTRESS (MEAN REMOVED)
MONTH
LONGTITUDE
1 m/s

$\tau^{y'}$

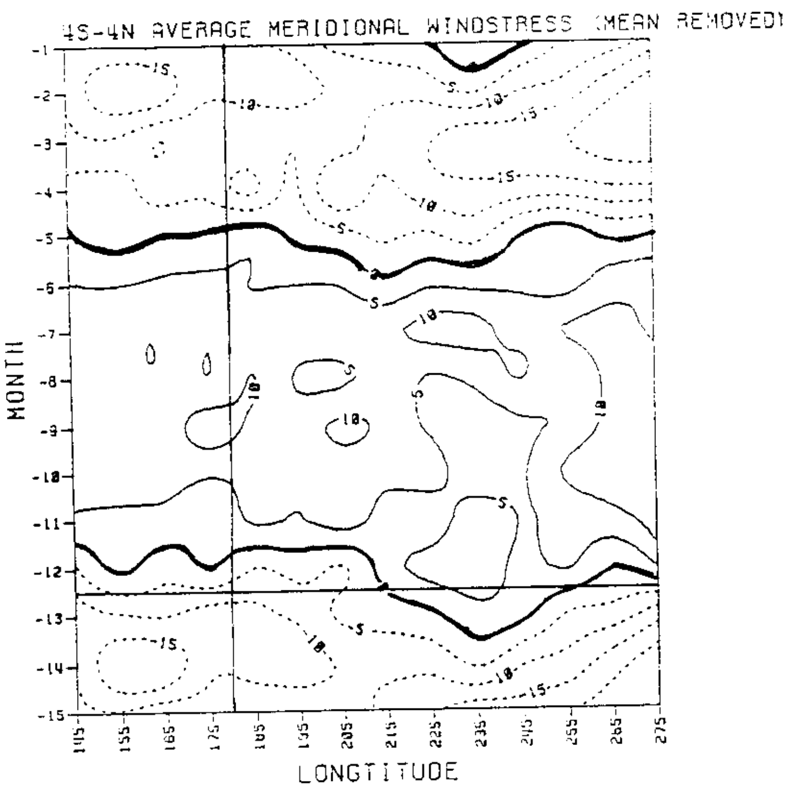

4S-4N AVERAGE MERIDIONAL WINDSTRESS (MEAN REMOVED)
MONTH
LONGTITUDE

Equatorial Sverdrup Balance (Wyrtki, 1984)

- $\tau^x/H = \delta\eta/\delta x$
- 1-1/2 layer model, no motion at all
- sea surface slopes up to the west
- thermocline slopes down to the west
- effective depth, H, not well-defined
- depends strongly on factors controlling τ^x
- ignores equatorial waves and adjustment to variable forcing

Walker Circulation (Cornejo-Garrido & Stone, 1977)

- coupled ocean-atmosphere-land phenomenon
- strength and location variable
- depends on strength and position of diabatic heat source(s) over Maritime Continent region for moisture convergence (positive feedback)

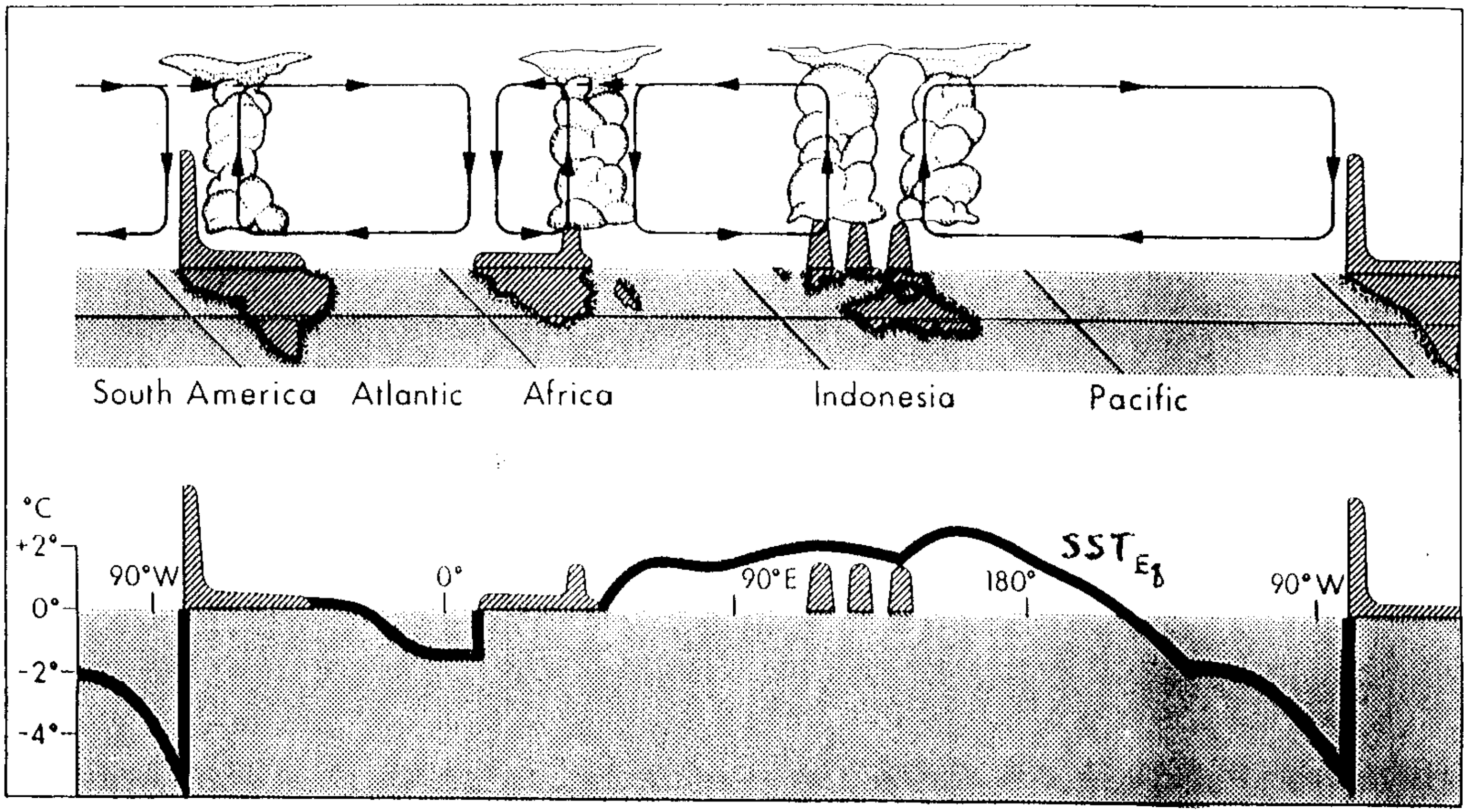

Figure 3. The Walker circulation along the equator, resulting in rising air and heavy rains over Indonesia, Africa and Brazil. Its strongest branch over the Pacific is related to the sea surface temperature; it is warm where air is rising and cool where air is sinking.

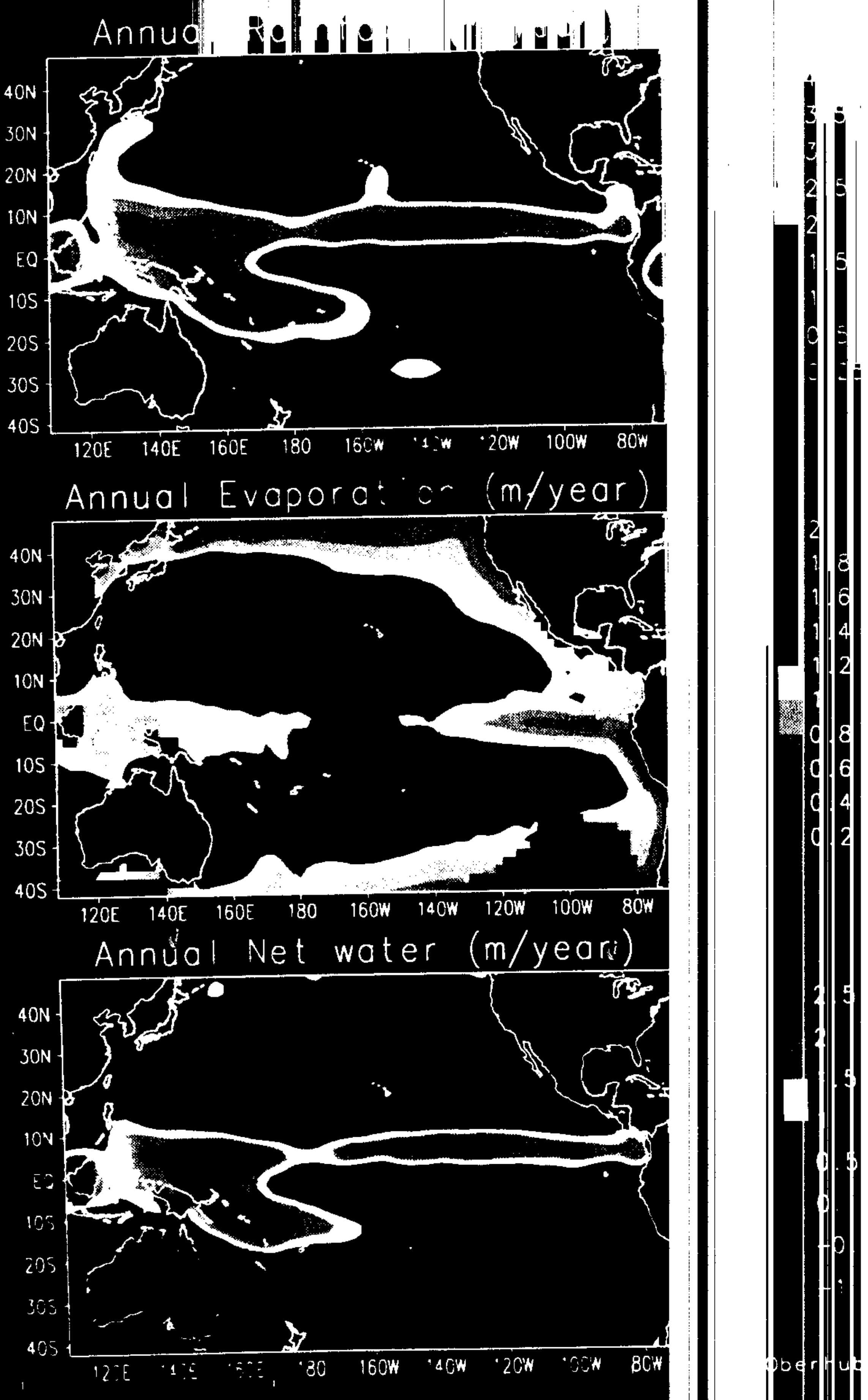
40N
30N
20N
10N
EQ
10S
20S
30S
40S
120E
140E
160E
180
160W
120W
100W
80W
Annual Net water (m/year)

ENSO

- requires zonal slope of equatorial thermocline (upwelling mode)
- requires zonal gradient of equatorial SST (SST mode)
- period of unstable oscillation depends on magnitude of one or both of these (Hirst, Battisti & Hirst, Neelin, Jin, etc..)

ENSO

- coupled ocean-atmosphere sensitivity to prescribed external convective heat source (Anderson & McCreary, 1985; Masumoto and Yamagata, 1989)
  - intense convection ==> stronger Walker circulation
    ==> stronger along equator gradients
    ==> longer period between ENSO events
  - what are the factors which determine the strength of this convection?

Masumoto + Yamagata (1991)

Anderson + McCreary (1985) model

Rossby waves are damped. Unstable coupled Kelvin mode is dominant

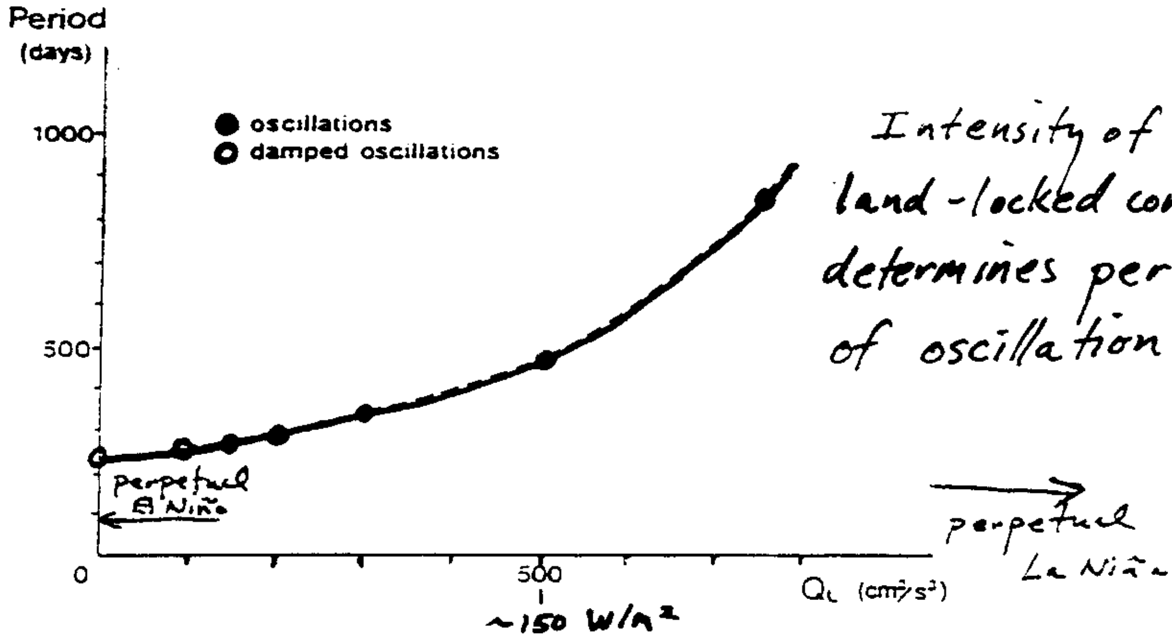

Intensity of land-locked convection determines period of oscillation

Fig. 4. Period of oscillations as a function of the amplitude of land heating Q_L.

Zonal wind stress (easterly shaded)

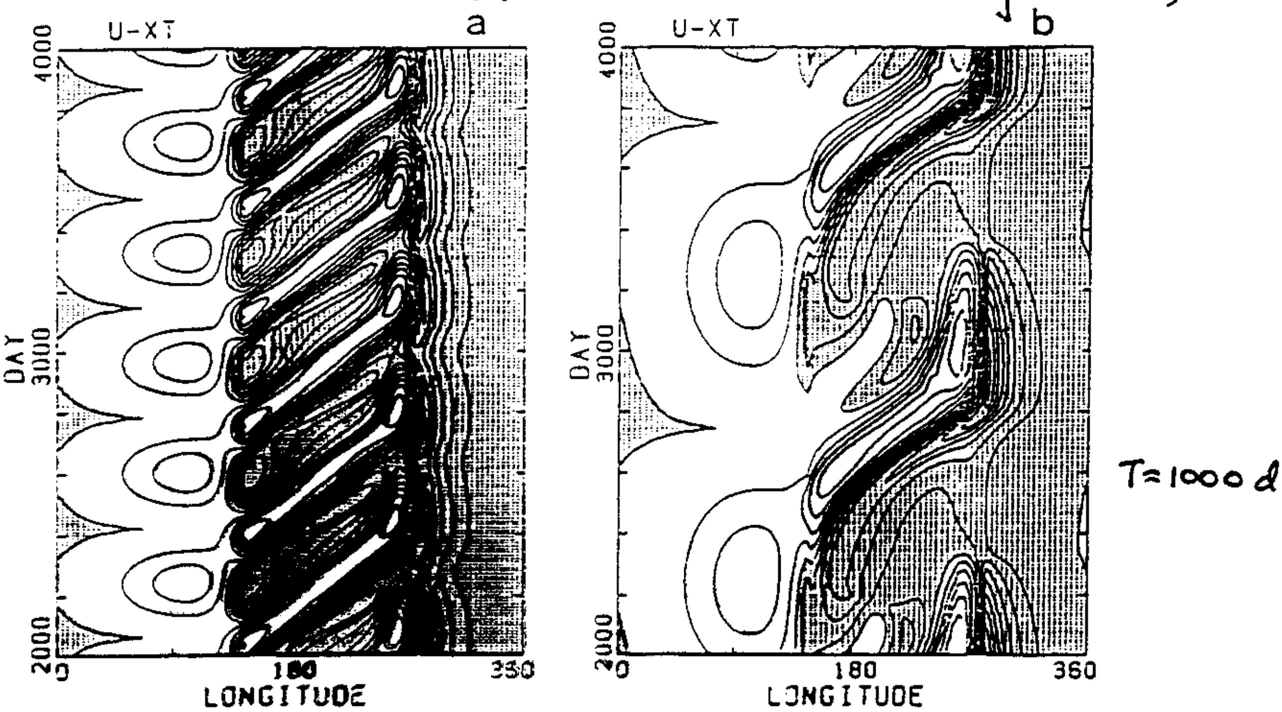

Fig. 5. As in Fig. 2 except for the case with oscillatory heating over land. a) Period is 360 days. b) Period is 1000 days.

$Q_L = 500 + 500 \sin(2\pi t/T)$ cm²s⁻³

Interaction between zonal and meridional circulations

- meridional migration of 'land-locked' monsoonal heat sources
- ENSO zonal migration of W. Pacific warm pool heat source
- competition between land-locked and oceanic convection

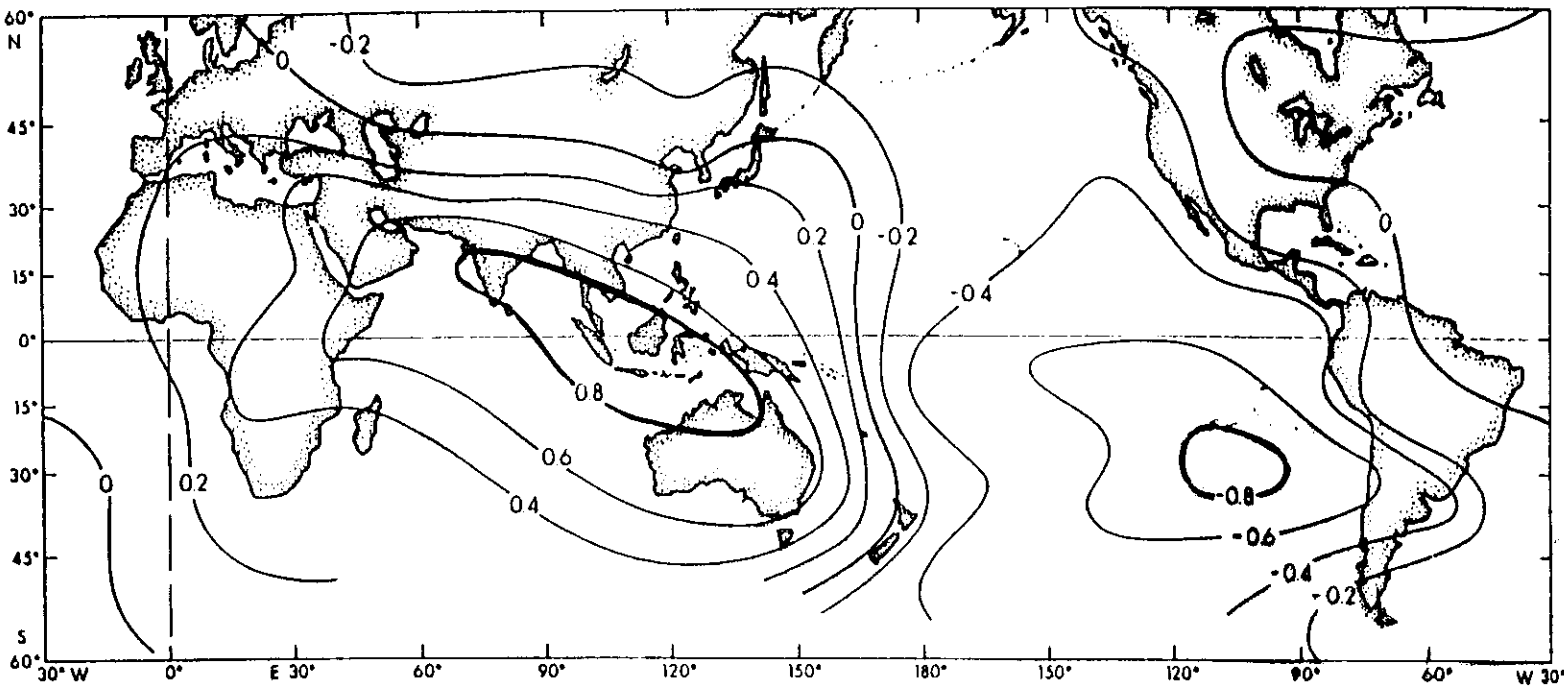

Figure 1. The southern oscillation. Correlation of annual mean atmospheric pressure with Jakarta (after Berlage).

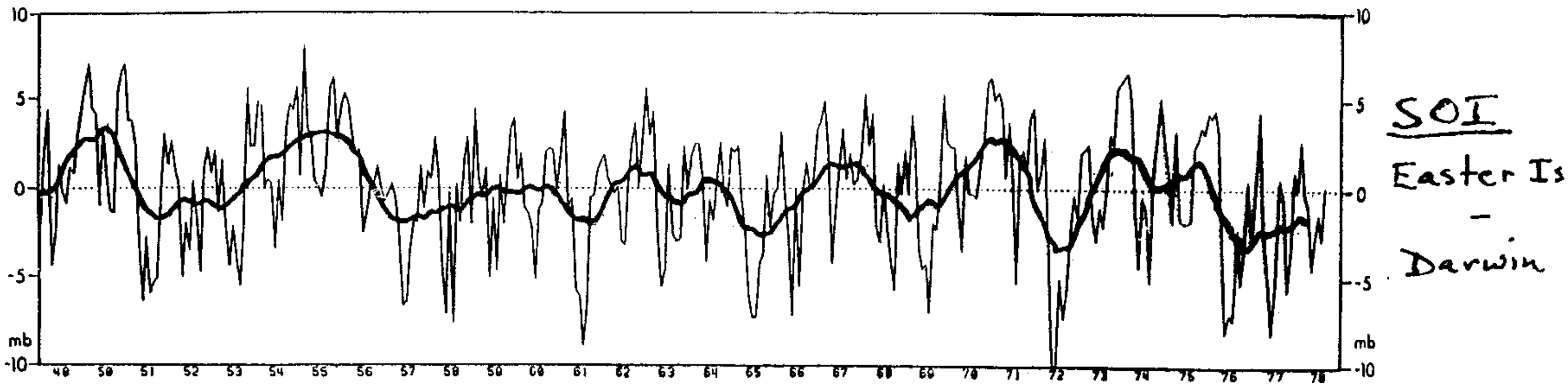

Figure 2. The Southern Oscillation as given by the difference of atmospheric pressure between Easter Island and Darwin, Australia from 1949 to 1978 relative to a mean of 10.3 millibars. The thin line gives monthly means, the heavy line the 12-month running mean.

Trenberth + Soloman (1994)

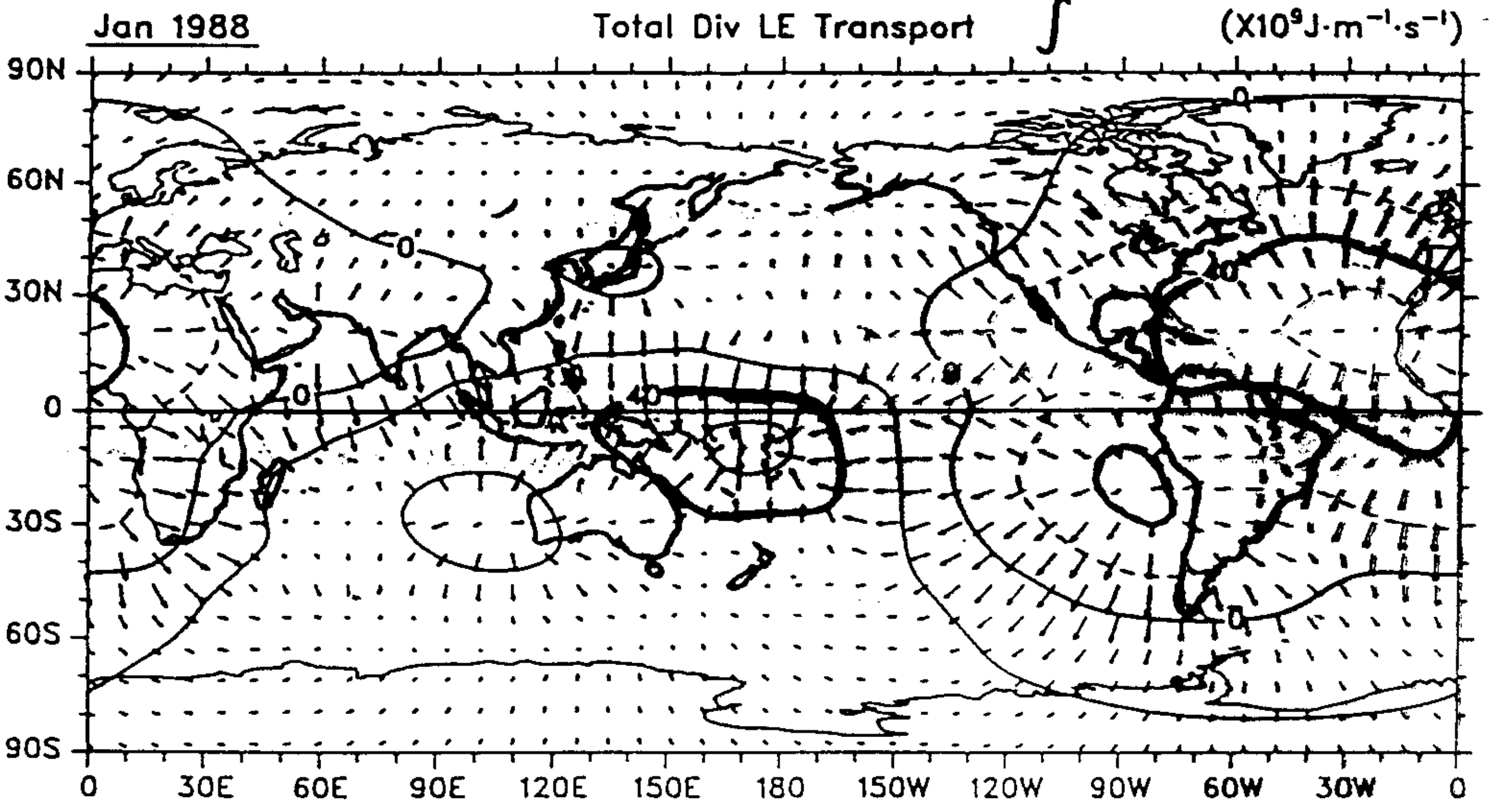

contours × 10^{13} $J s^{-1}$ SCALING VECTOR ⟶ 0.4 *~ 40 × 10^{13} $J s^{-1}$*

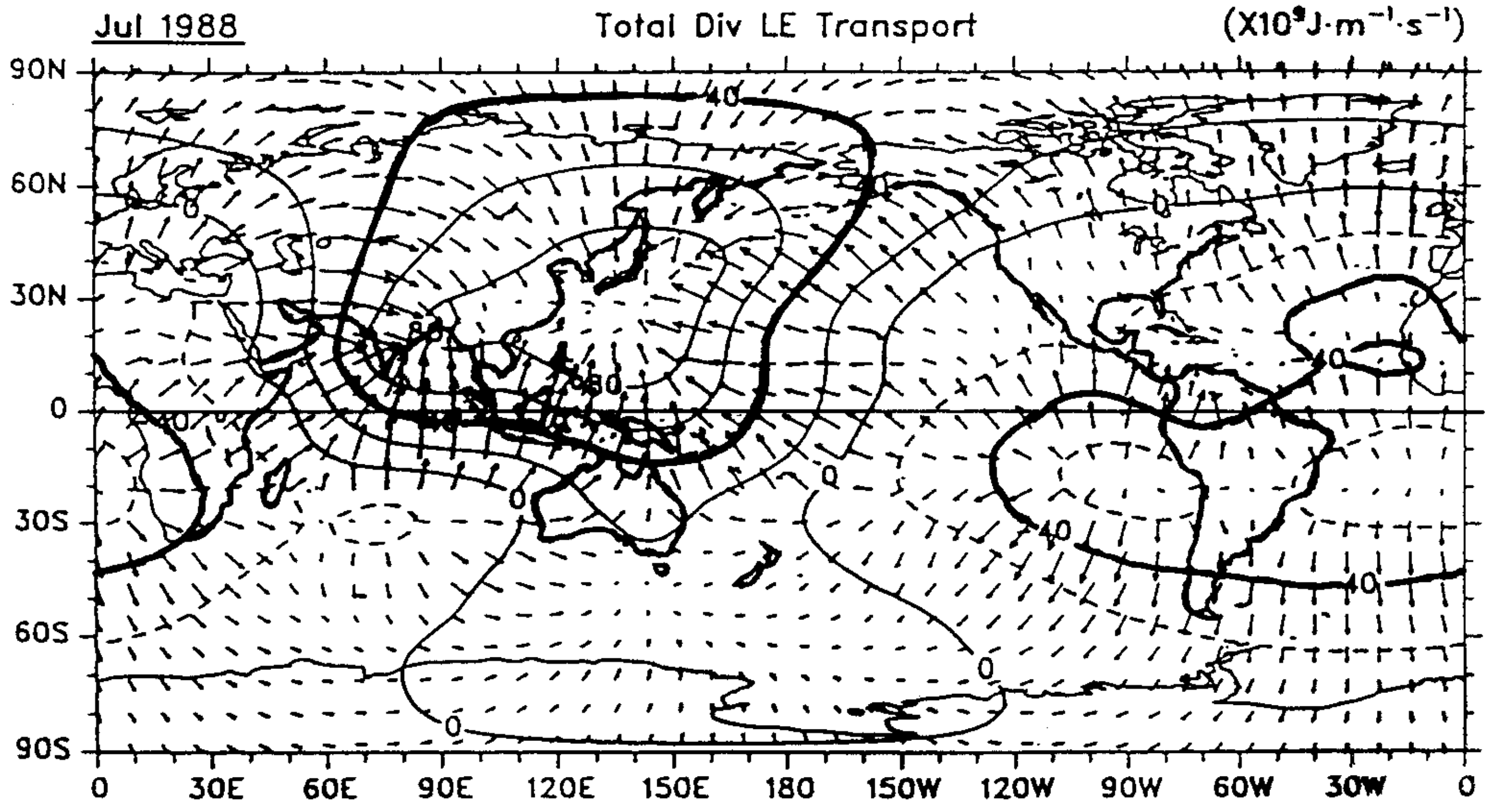

SCALING VECTOR ⟶ 0.4

March SST

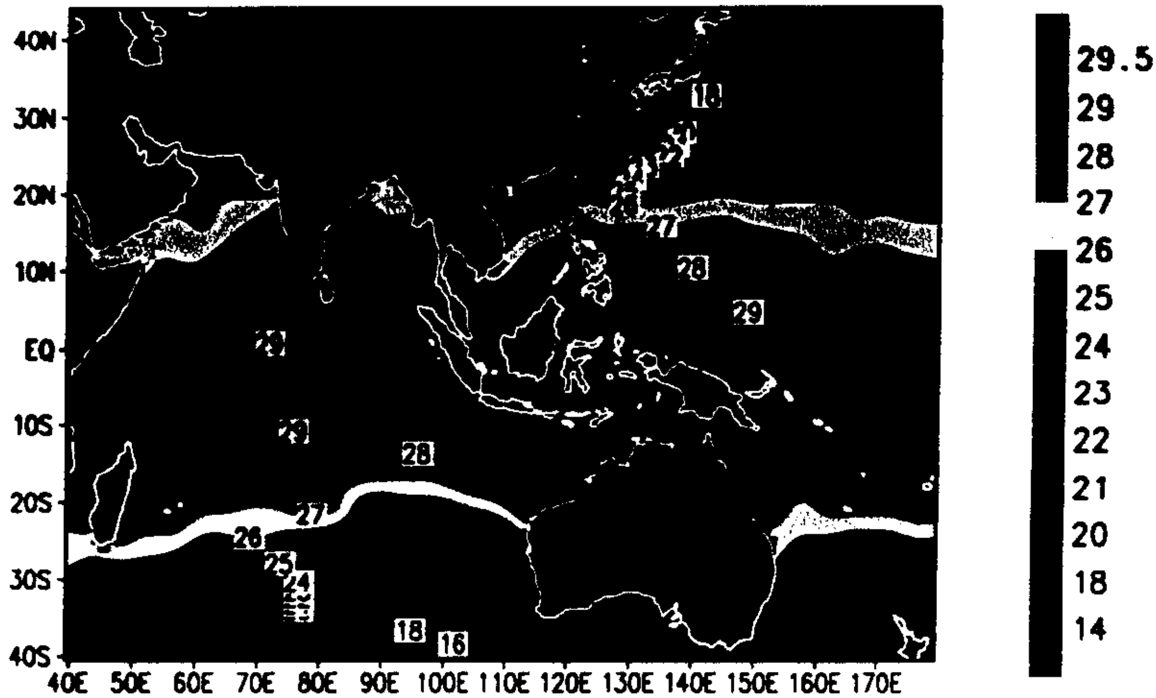

September SST

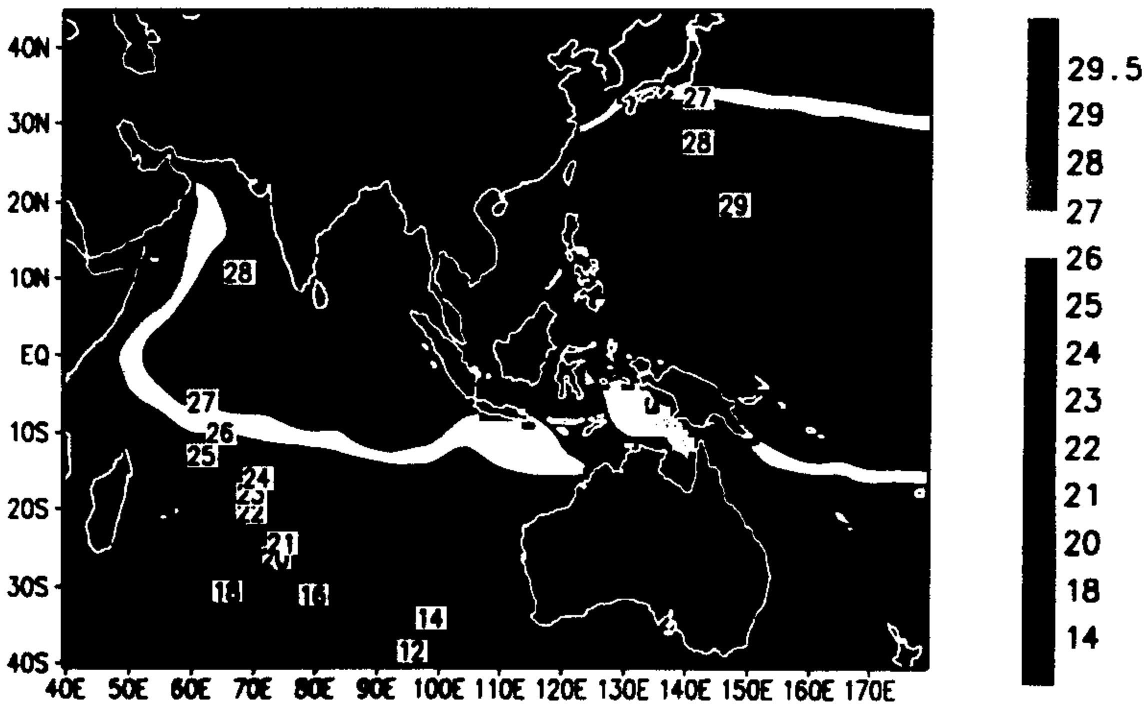

CAC Annual SST - 1992

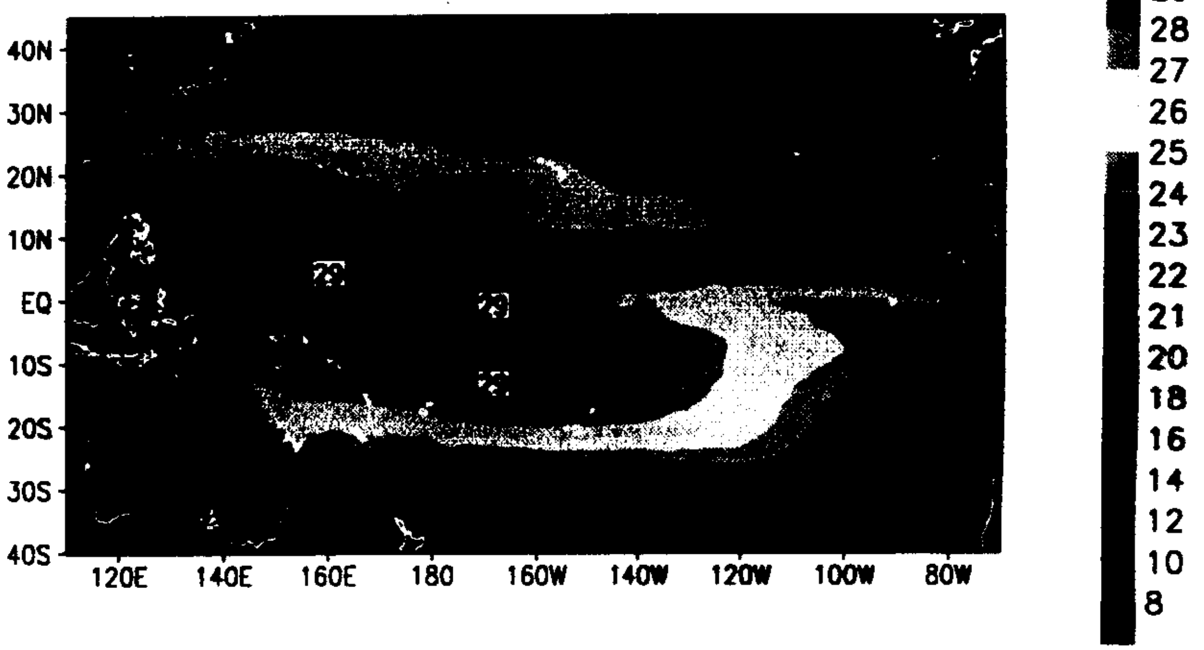

Depth of the 29°C isotherm

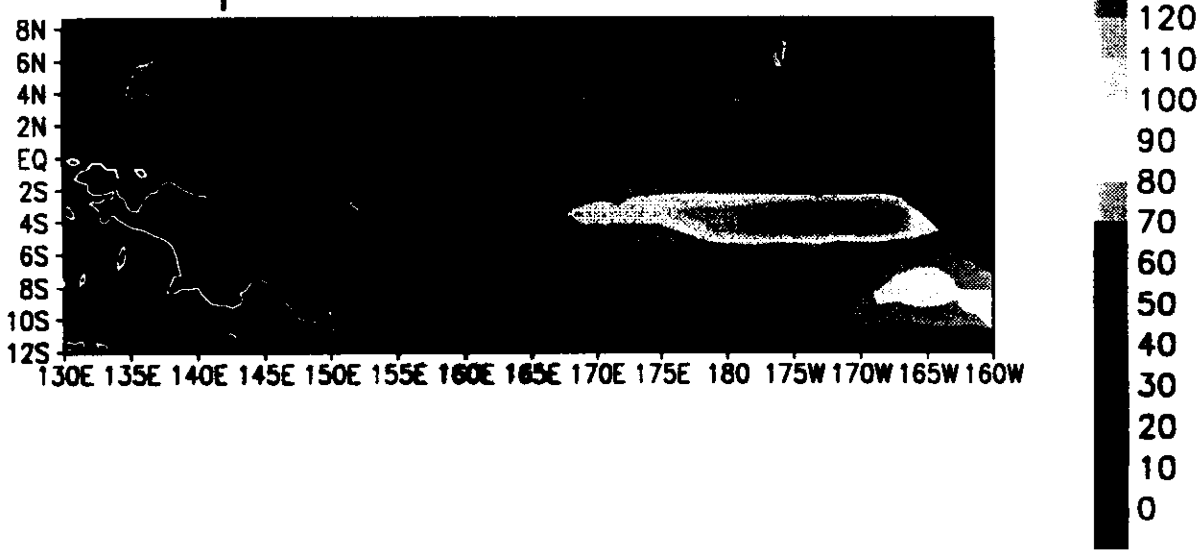

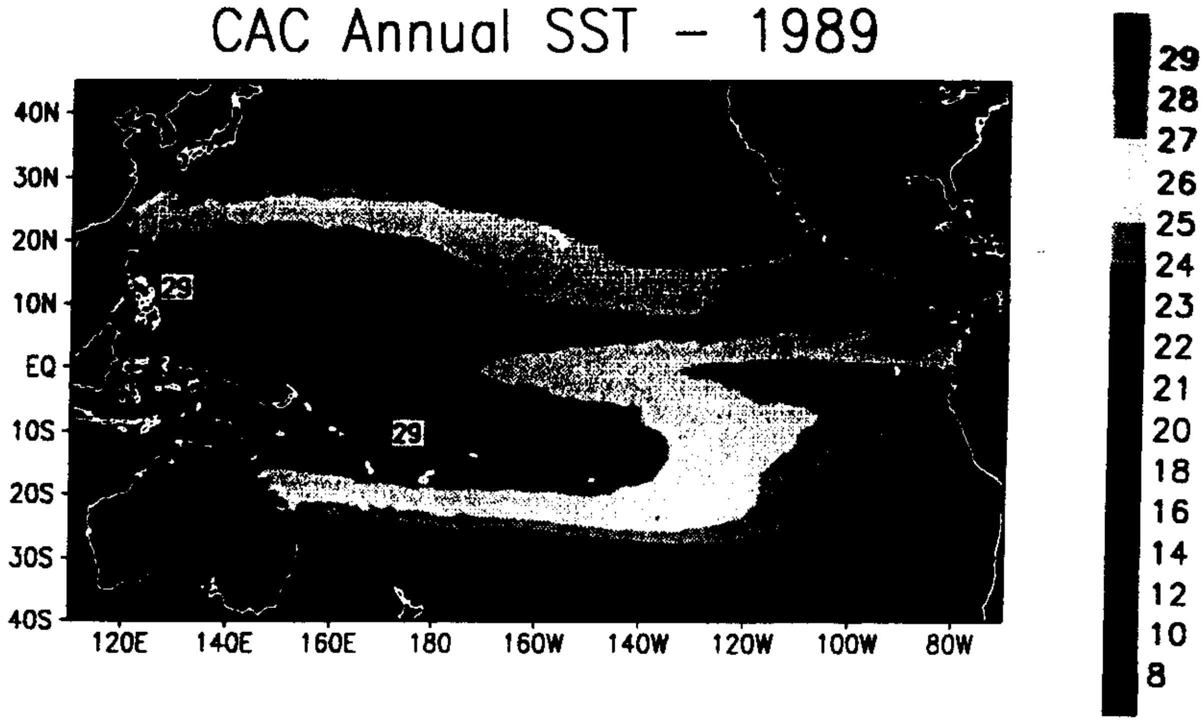

CAC Annual SST - 1989
40N
30N
20N
10N
EQ
10S
20S
30S
40S
120E
140E
160E
180
160W
140W
120W
100W
80W
29
29
28
27
26
25
24
23
22
21
20
18
16
14
12
10
8

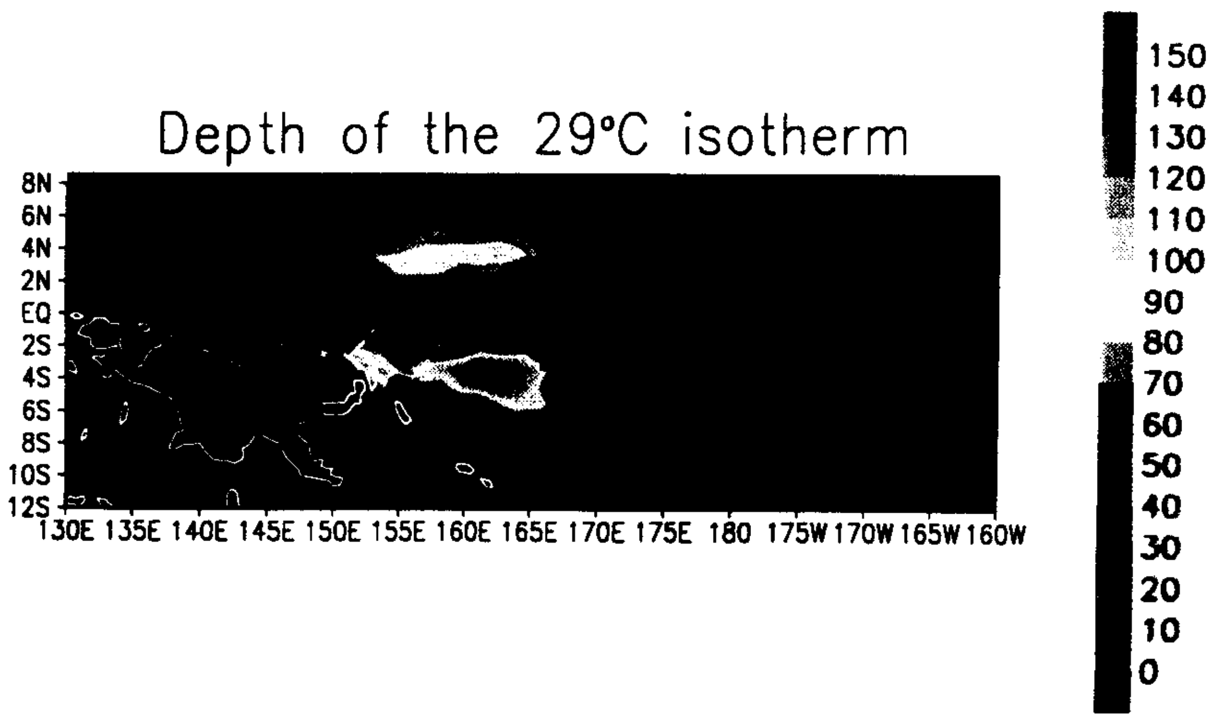

Depth of the 29°C isotherm
8N
6N
4N
2N
EQ
2S
4S
6S
8S
10S
12S
130E 135E 140E 145E 150E 155E 160E 165E 170E 175E 180 175W 170W 165W 160W
150
140
130
120
110
100
90
80
70
60
50
40
30
20
10
0

East edge of warm pool along Equator
(28.5°C)

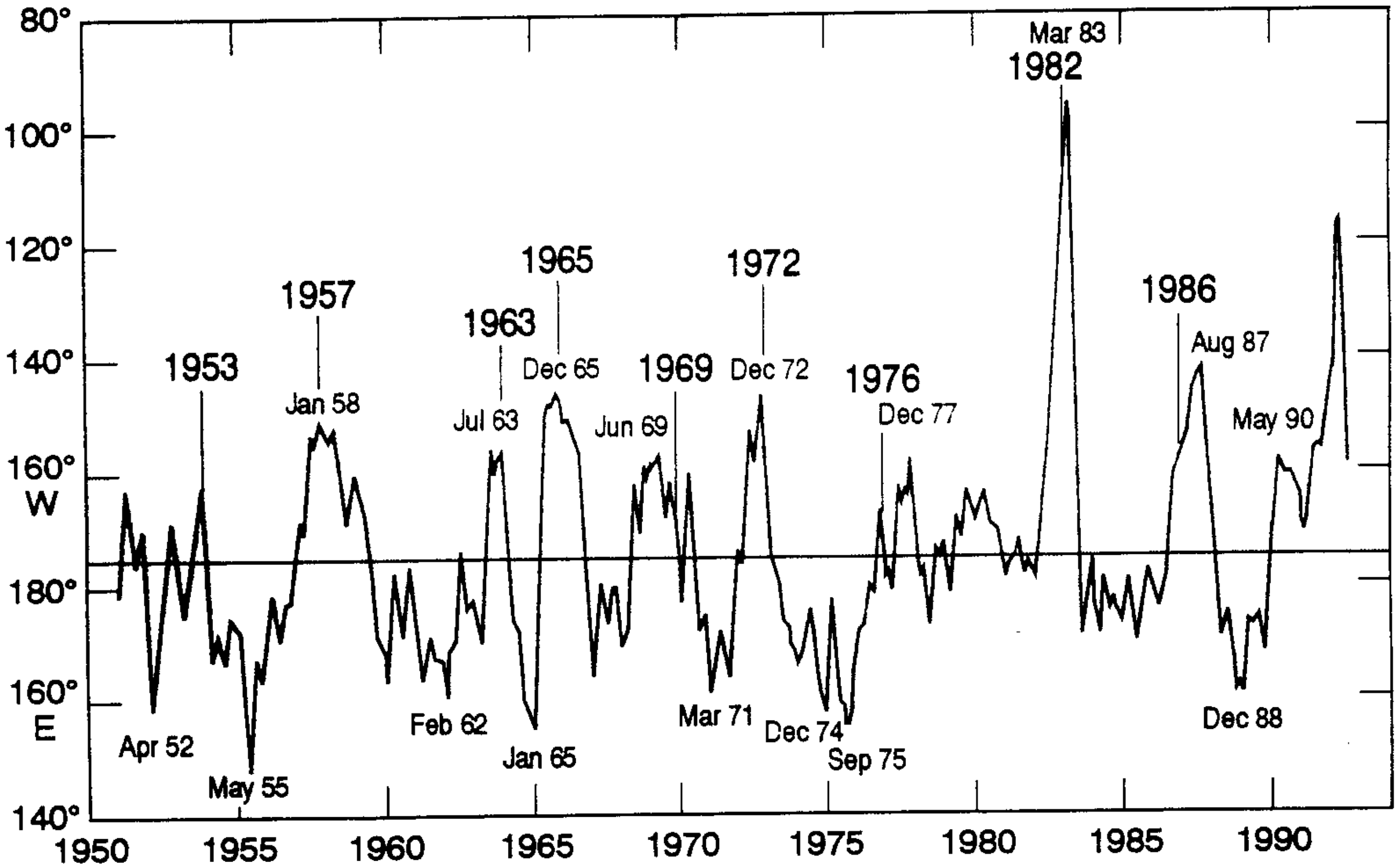

courtesy of P. Webster (PAOS/CU)

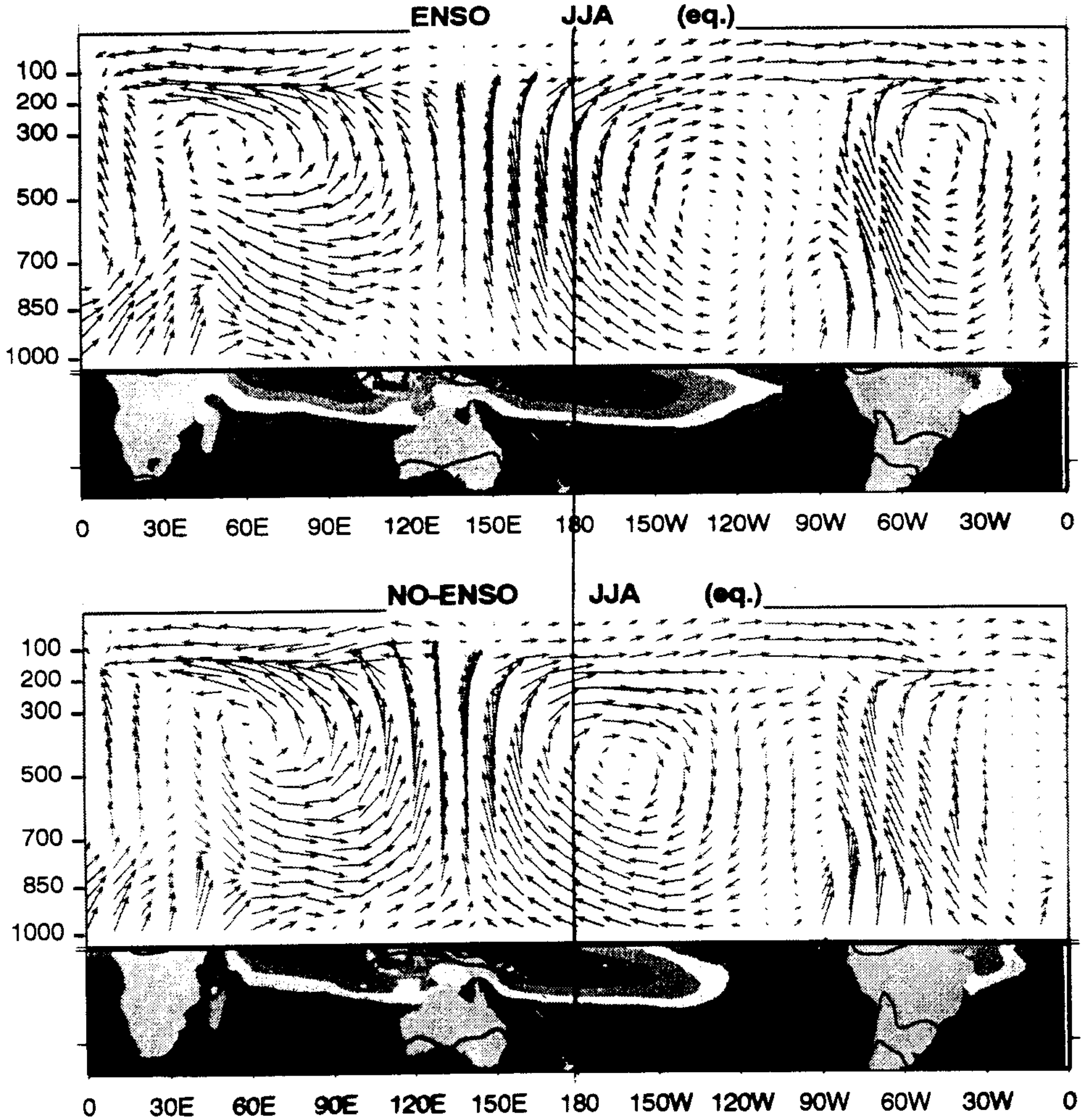

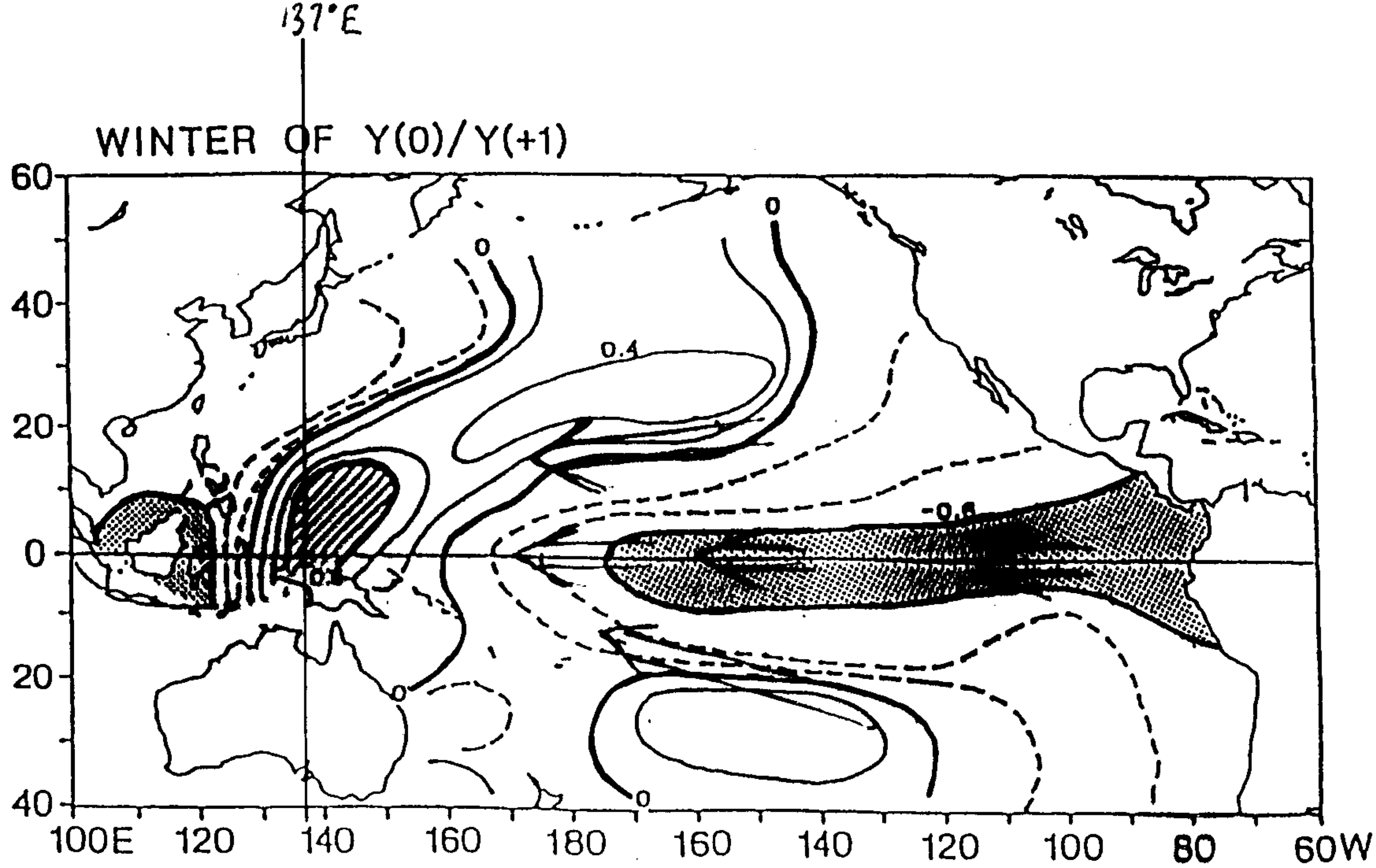

SST correlation with preceding Indian monsoon rainfall

heavy rains → strong Pacific trade winds → colder cold tongue
warmer warm pool

Yasunari (1990)

Meehl (1993)

OCEAN TEMPERATURE PROFILES, NORTH NEW GUINEA

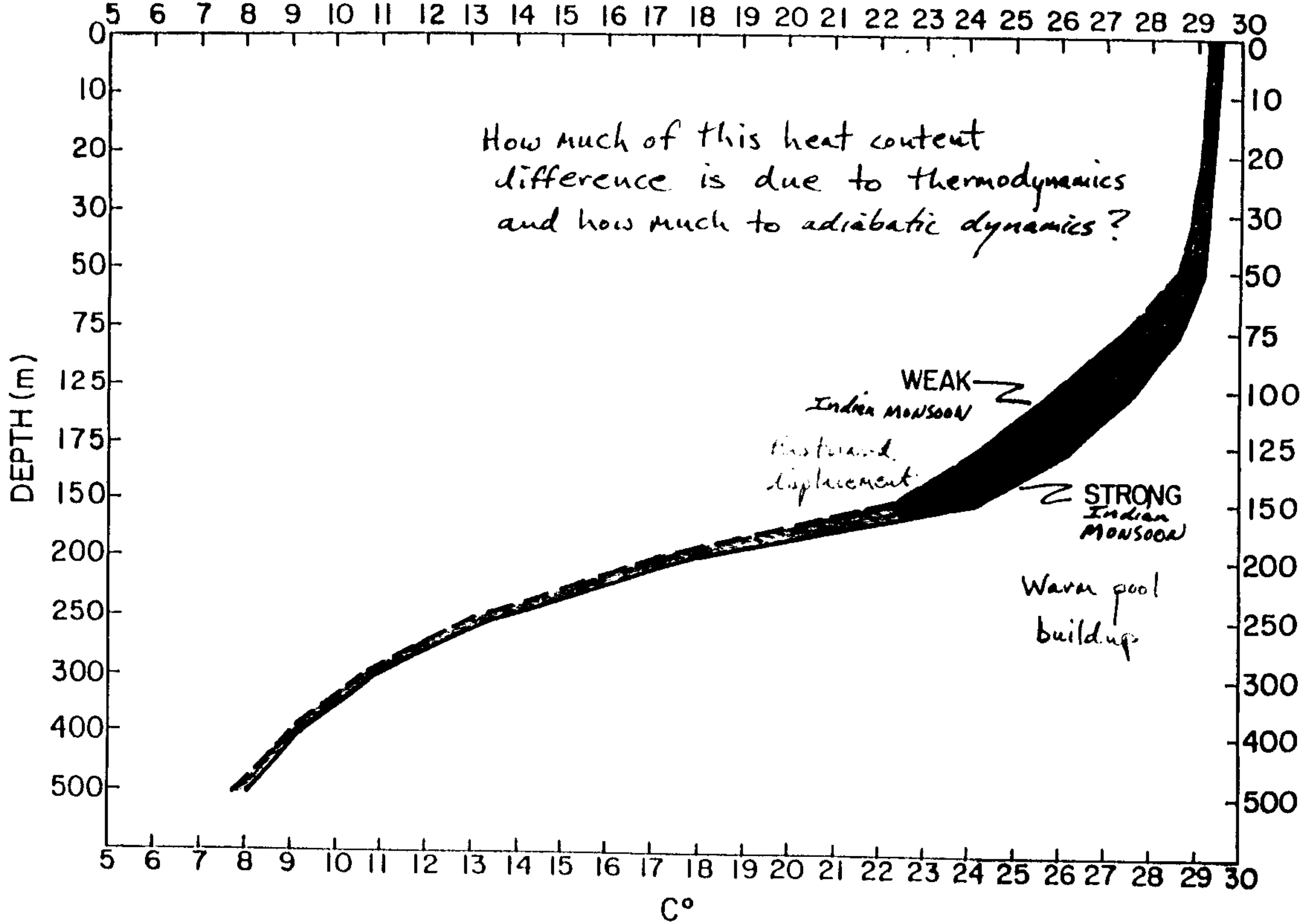

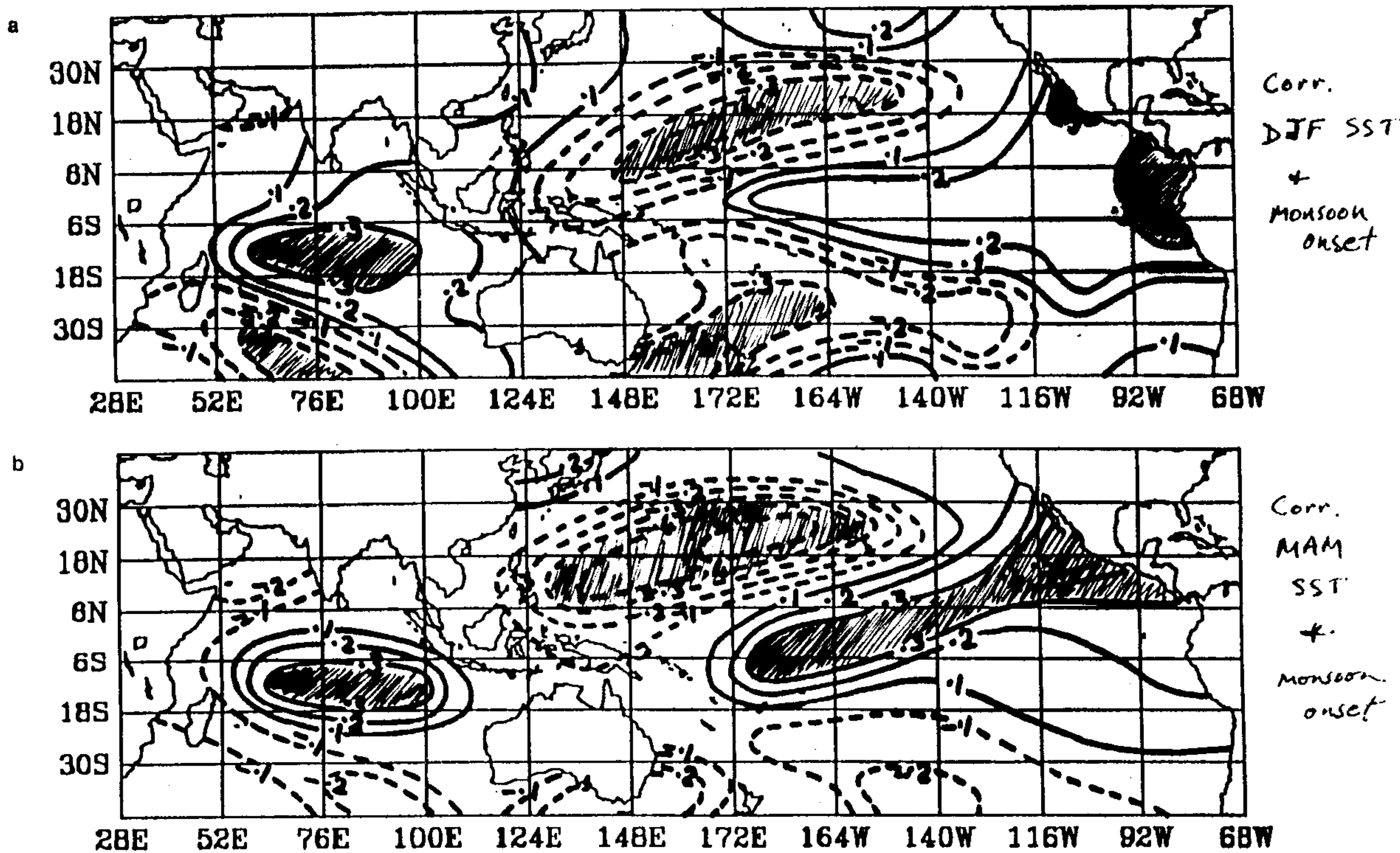

FIG. 11. Isopleths of correlation coefficient between the seasonal SST anomaly in each 12-degree latitude by 24-degree longitude box and the following MOK for (a) the December–February season, and (b) the March–May season. Isopleths are at 0.1°C intervals (0°C line not marked), positive by continuous lines and negative by broken lines.

Asian summer Strong monsoon years : SST anomaly for MAM composite

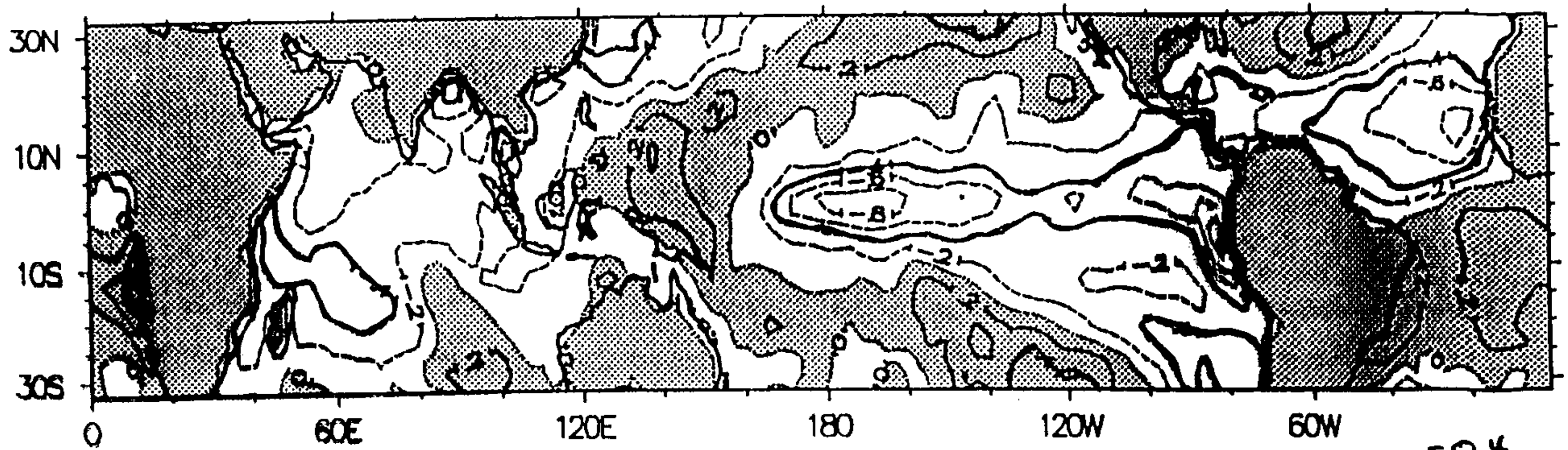

-0.4

Ju + Slingo (1996) Q. J. Roy. Met. Soc.

Asian summer Weak monsoon years : SST anomaly for MAM composite

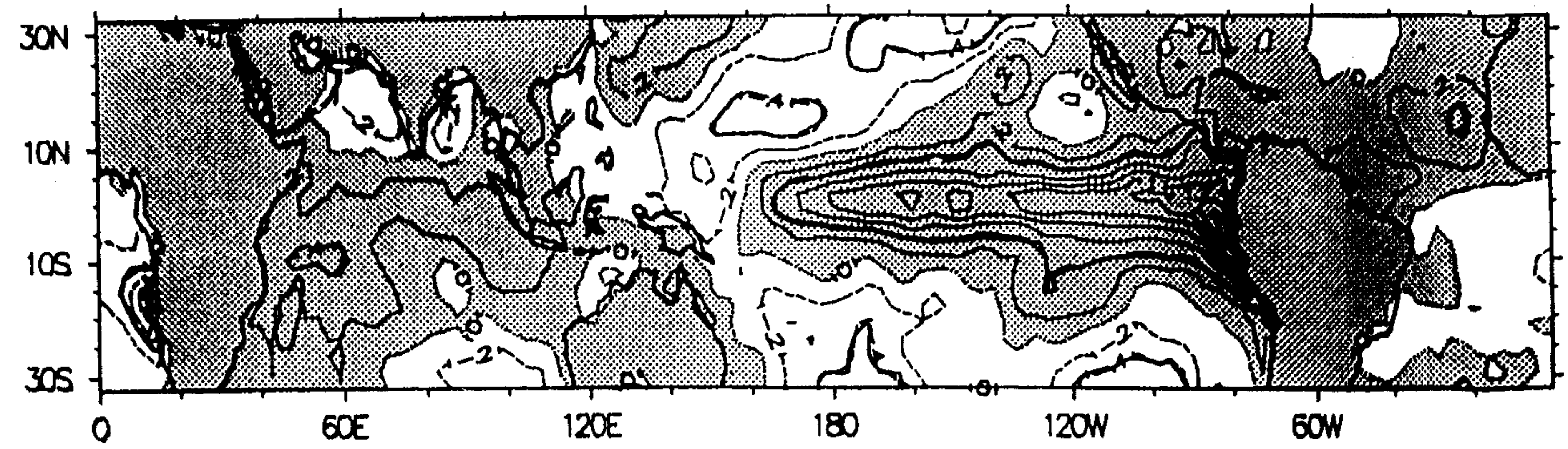

Metzger + Hurlburt (1996)

wind stress H+R winds curl τ

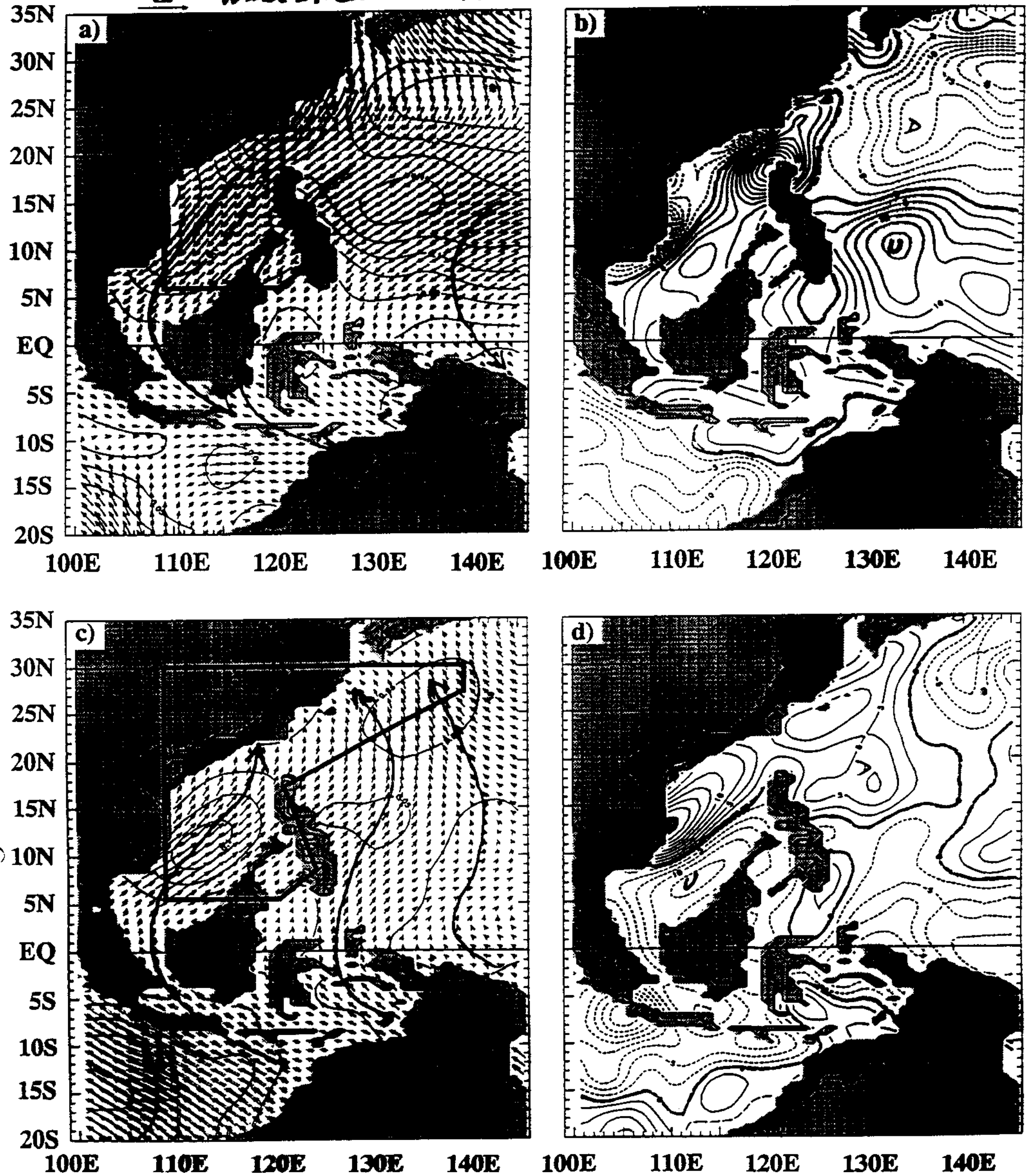

FIG 2

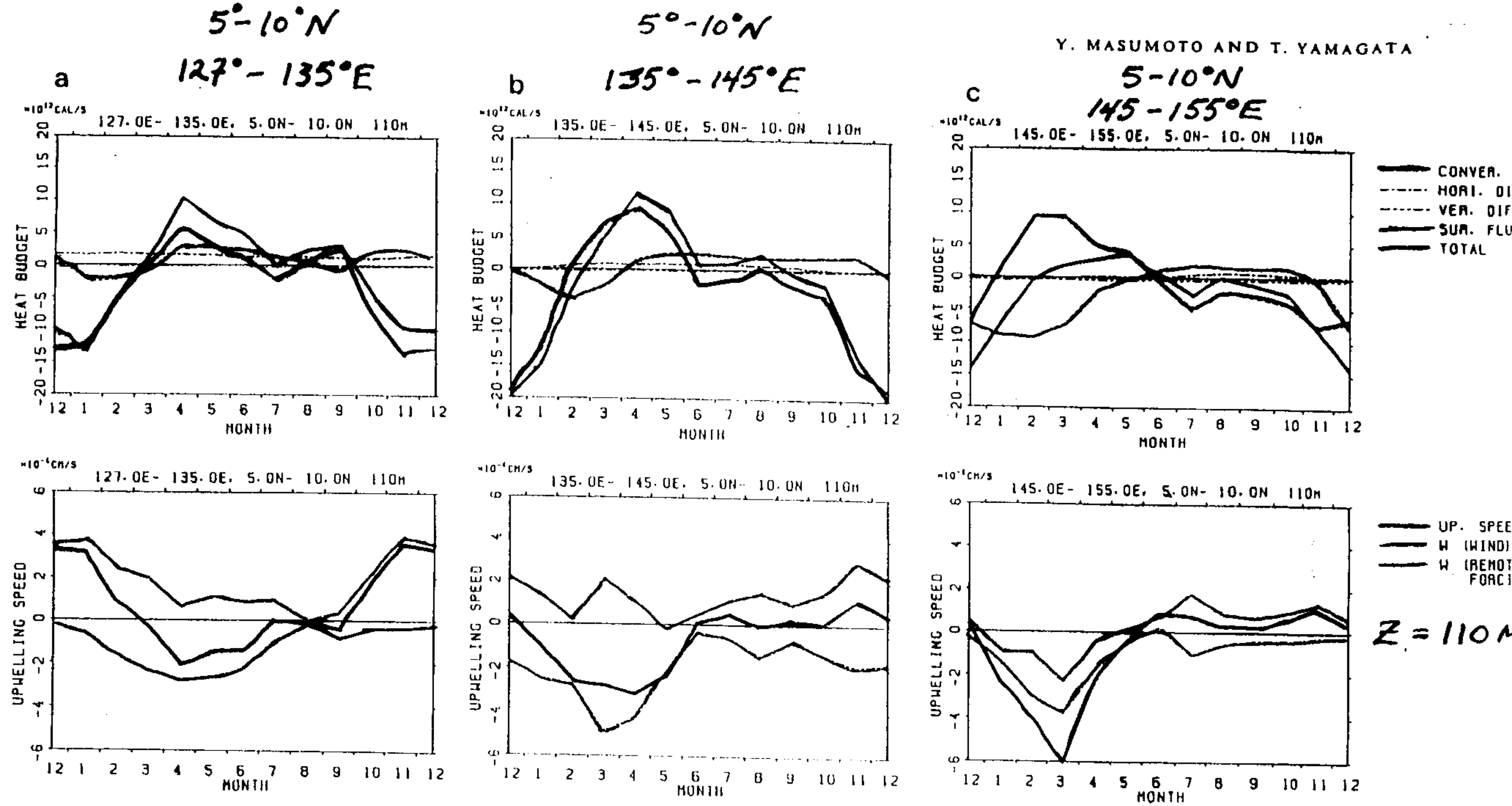

FIG. 10. Monthly mean heat budget analysis for (a) Box A, (b) Box B, and (c) Box C. The rate of change of heat storage is determined by the convergence of heat transport, flux across the surface, and horizontal and vertical diffusion. The modeled upwelling speed (in 10^{-4} cm s^{-1}) at a depth of 110 m, the contribution from the Ekman pumping (due to local wind forcing), and the difference between the two (due to remote forcing) are also shown. The modeled upwelling speed shows little vertical dependence in the surface mixed layor.

Sea Level

Station Locations

Mitchum + Lukas (1990)

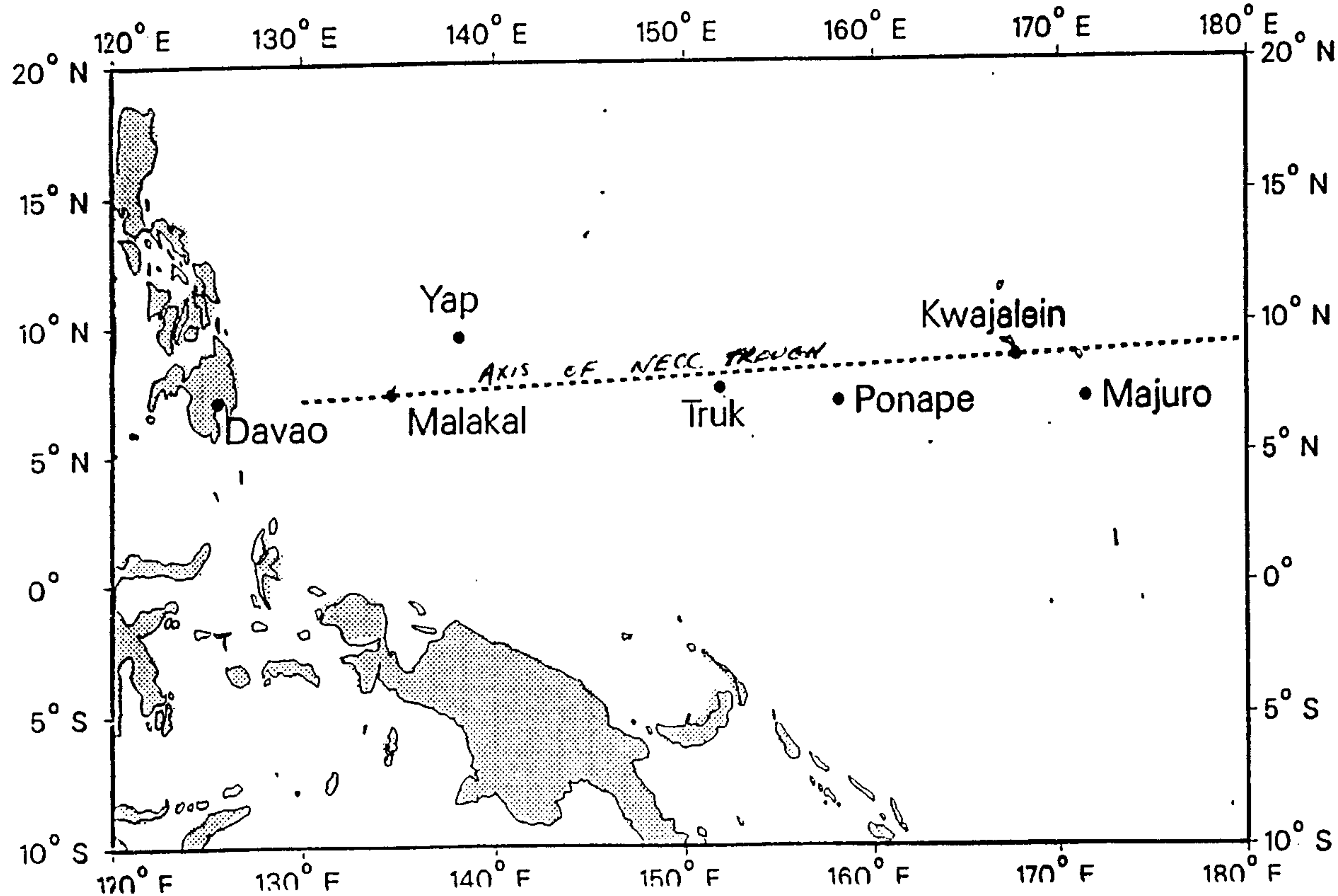

Fig 1

Mitchum + Lukas (1990)

W. Pacific – Sea Level near 7°N

Annual harmonics (from 11 years of data) at the 7 stations

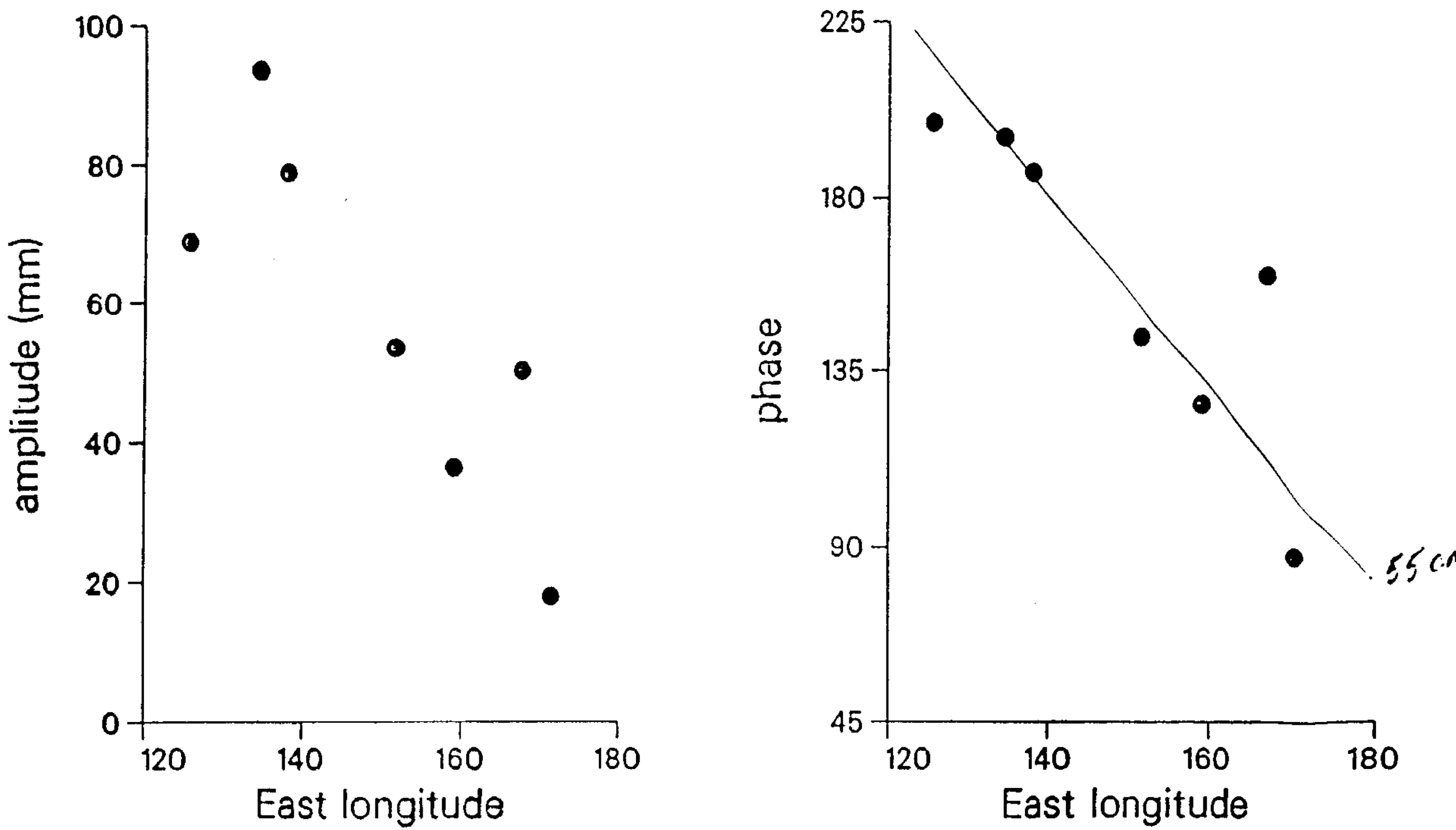

Fig 3

Results of amplitude and phase regressions

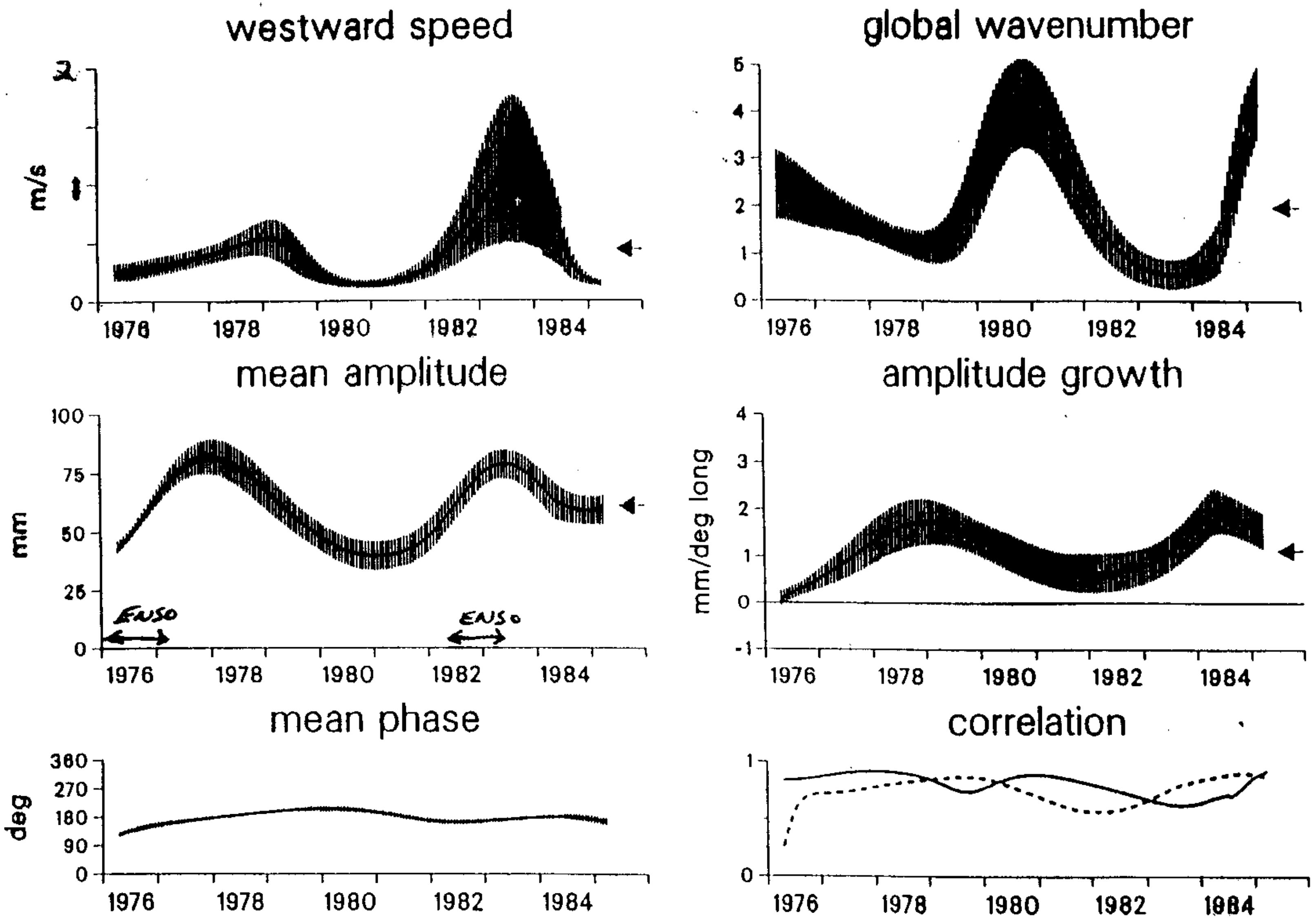

FIG. 5. Summary of amplitude and phase regressions based on the complex demodulation analysis. Details of the calculations are given in the text. The westward speed is inversely proportional to the phase gradient with longitude. The global wavenumber is inversely proportional to the phase speed and is in units of cycles per Earth circumference. The amplitude growth is positive if the amplitude is larger in the west. The error bars are ±one standard deviation, and the arrows at the right side of the four uppermost plots mark the average value.

Modulation of westward-propagating annual cycle *time-varying* amplitude

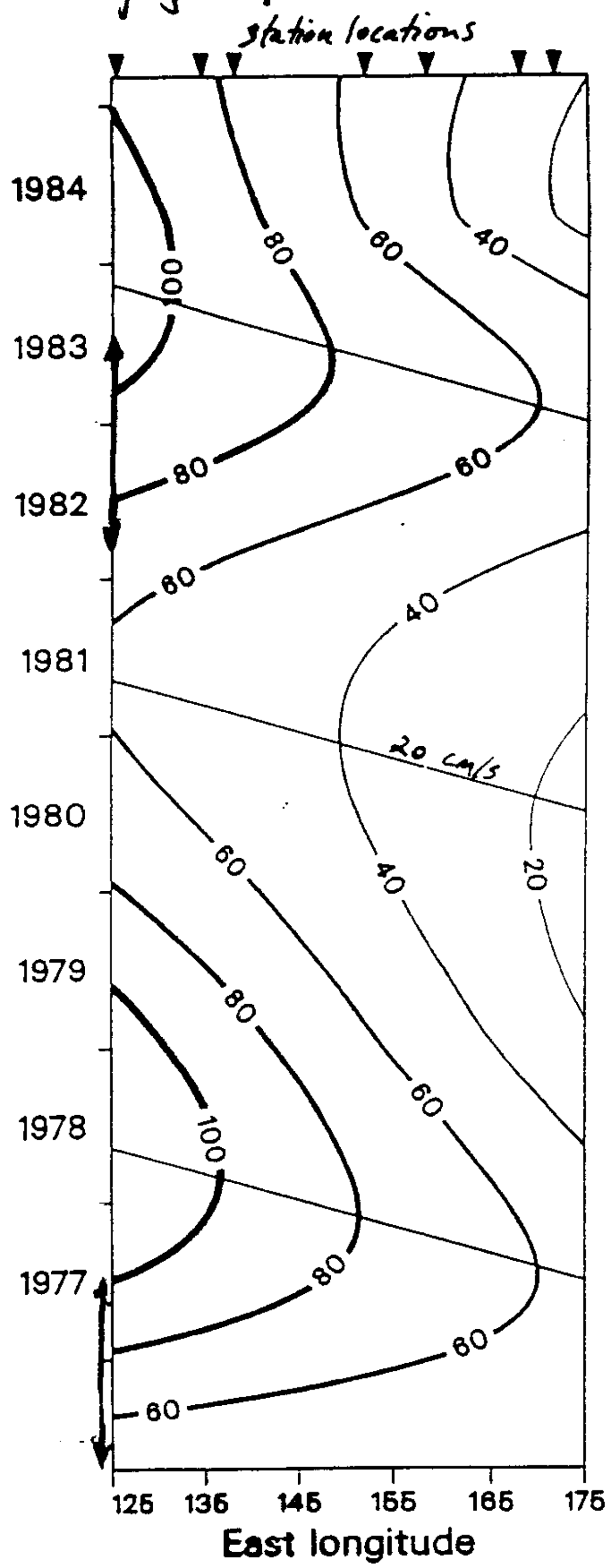

Mitchum + Lukas (1990

westward propagation of interannual modulation of annual cycle

FIG. 6. Description of the annual sea level amplitude versus longitude and time. The data contoured in this figure are constructed from the mean amplitude and amplitude growth time series shown in Fig. 5. The contours of the annual cycle amplitude are in millimeters. The arrows along the top edge of the plot show the locations of the stations where the sea level time series were measured. The three tilted lines indicate a propagation speed of 20 cm s^{-1}.

Minobe (1996)

Eddy SST (10°N–EQ)

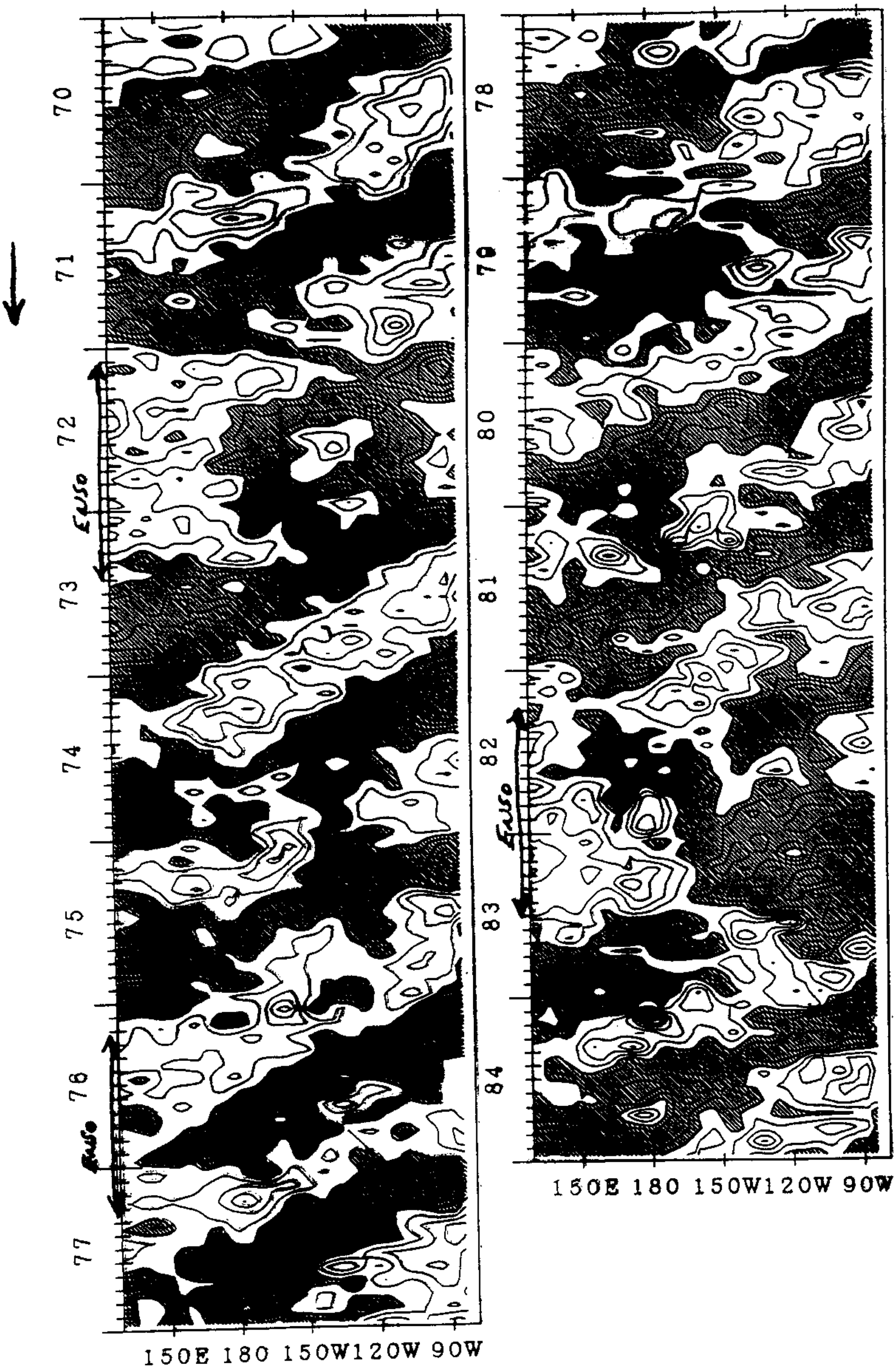

Eddy Meridional Wind Speed (8°N)

J. Climate

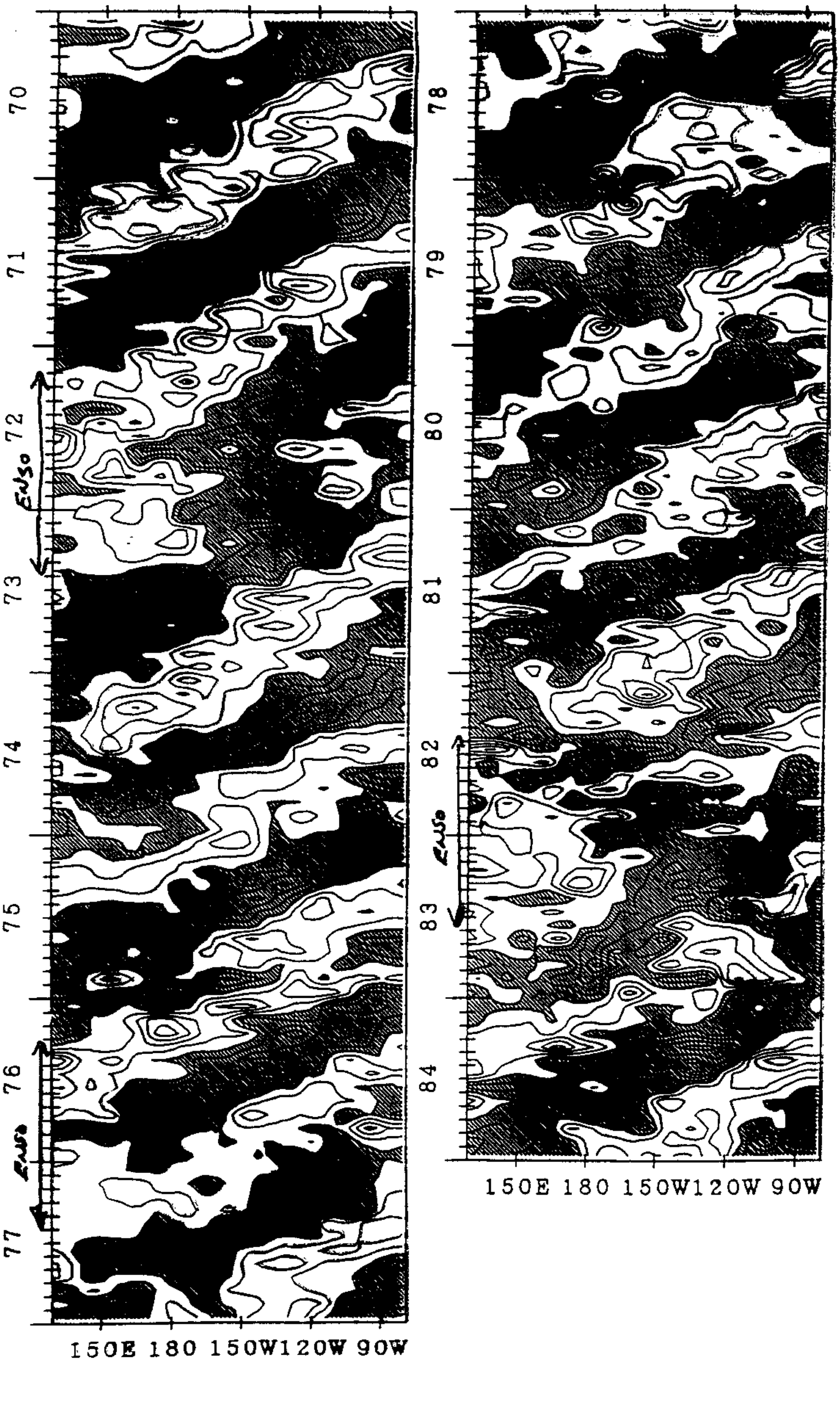

Fig.2

TOPEX Observations of Rossby Waves

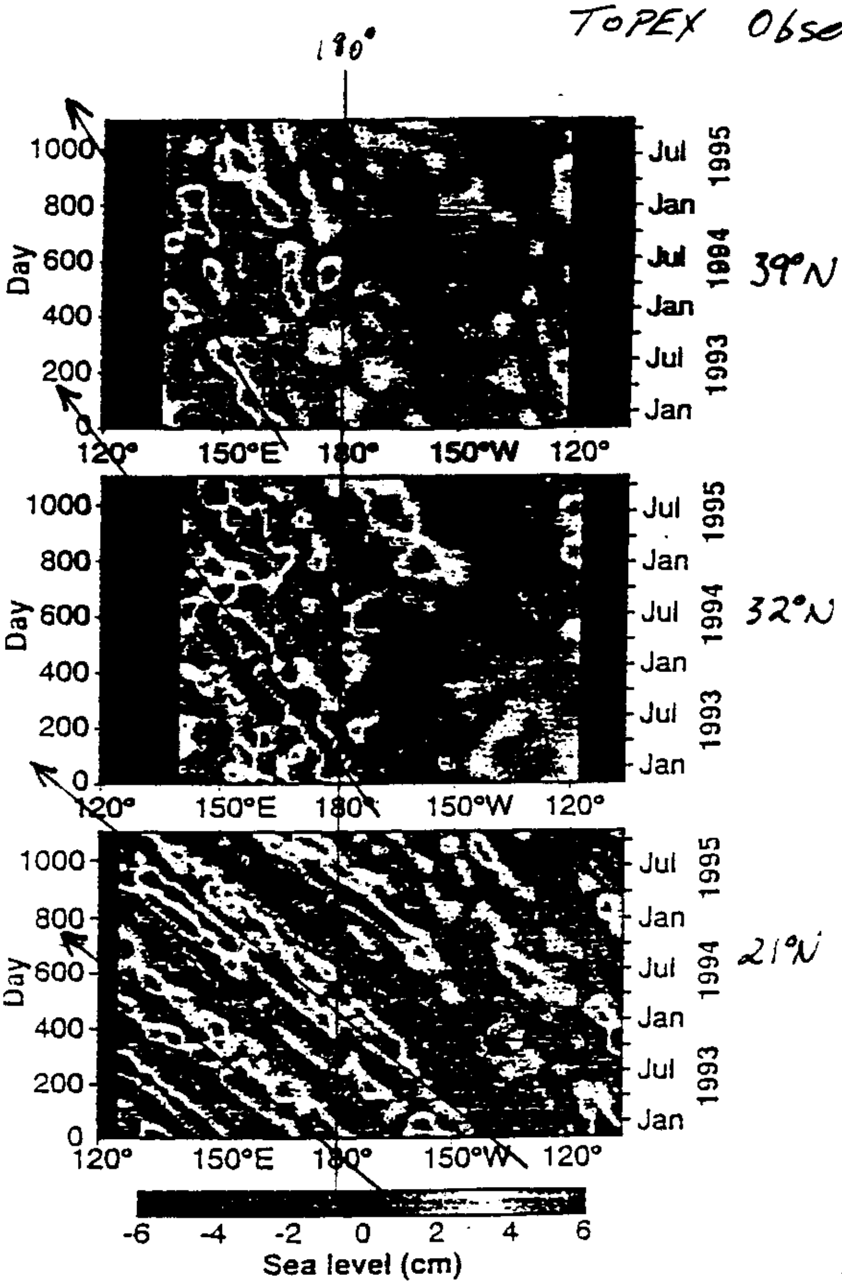

Fig. 2. Time-longitude sections of filtered sea level (22) in the Pacific Ocean along 39°, 32°, and 21°N. These examples are representative of extratropical latitudes throughout the world ocean.

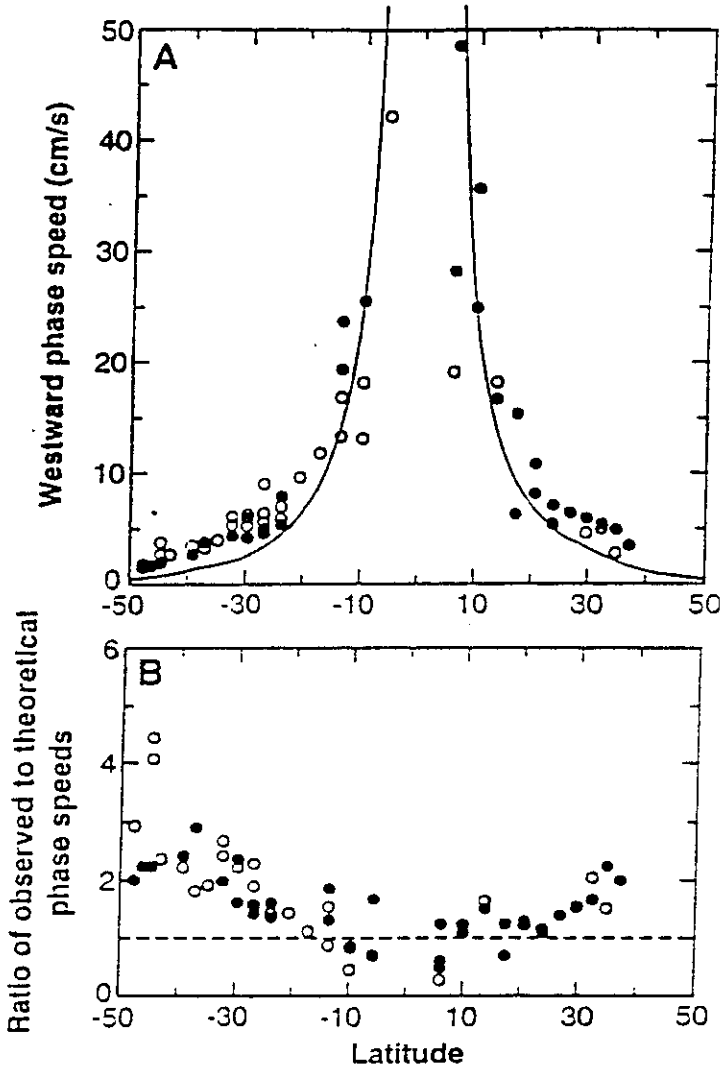

Fig. 5. (A) Globally distributed estimates of the phase speeds of westward-propagating sea level signals estimated from 3 years of TOPEX/POSEIDON altimeter observations. The solid circles correspond to Pacific estimates, and the open circles correspond to Atlantic and Indian Ocean estimates. The global average latitudinal variation of the phase speed predicted by the standard theory for extratropical freely propagating, nondispersive, linear, first-mode baroclinic Rossby waves (10) is superimposed as the continuous line. (B) Ratio of the observed phase speeds to the phase speeds predicted by the standard theory at the same geographical locations as the observations.

D. Chelton + M. Schlax

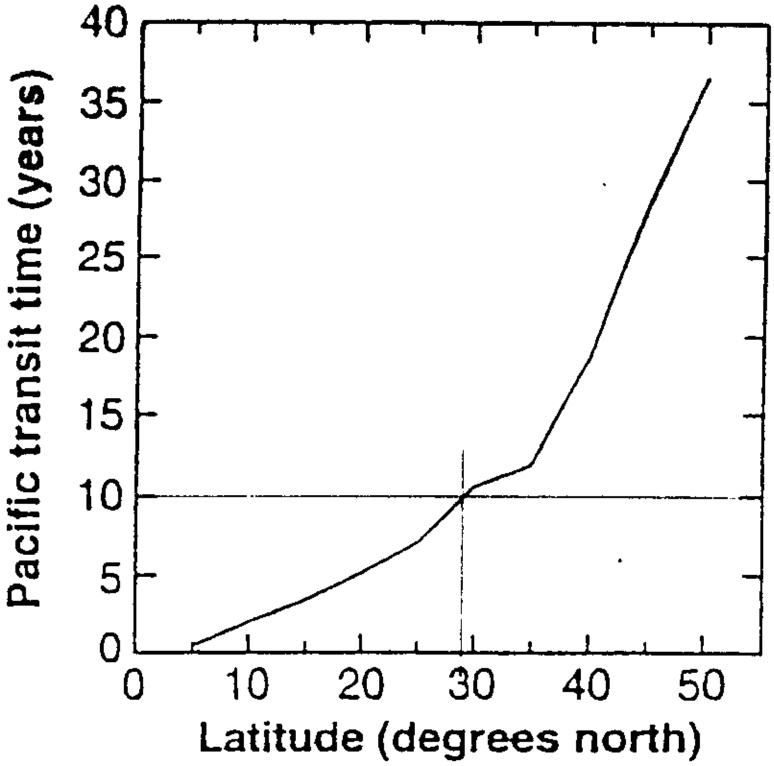

Fig. 1. Latitudinal variation of the time required for baroclinic Rossby waves to cross an ocean basin with the geometry of the North Pacific. These transit times are based on the phase speeds predicted by the standard theory for freely propagating, nondispersive, linear, first-mode baroclinic Rossby waves (*10*).

D. Chelton

Graham and White (1991, JPO)

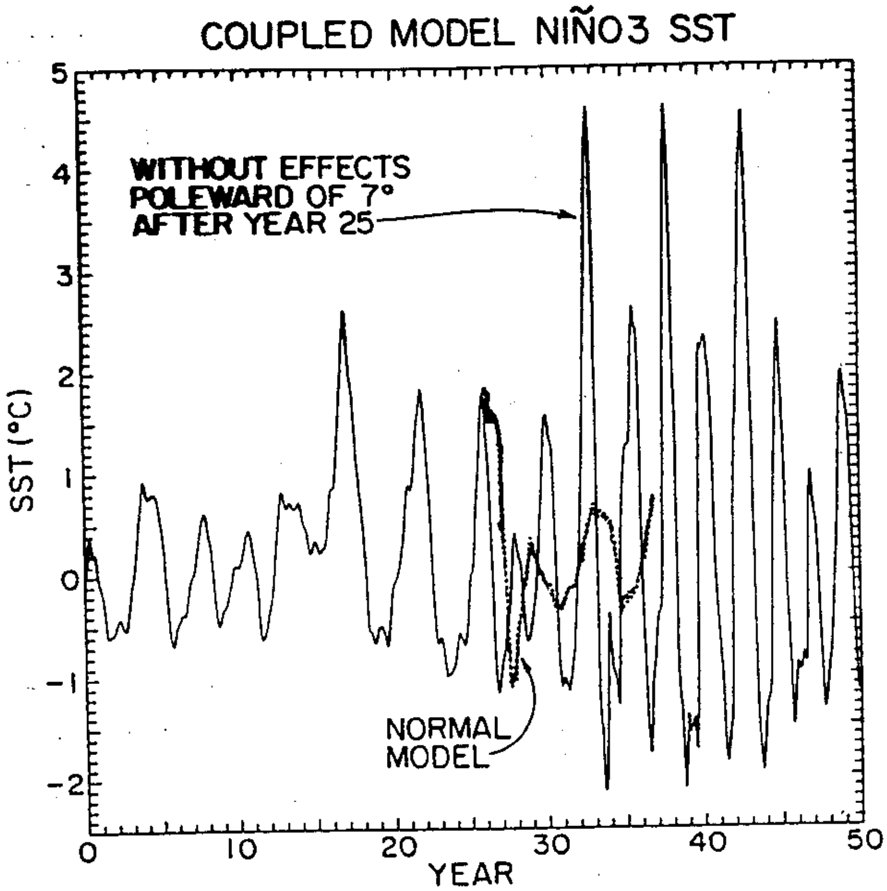

FIG. 5. Eastern Pacific SST anomalies from a simulation with the LDGO coupled model in which the outgoing Kelvin wave amplitude was calculated normally for the first 25 years and using the integrated zonal transport between 7°N and 7°S during the second 25 years (the change occurs at the tick mark indicating the beginning of year 25). The dotted line shows the results from an otherwise identical unmodified simulation with the coupled model.

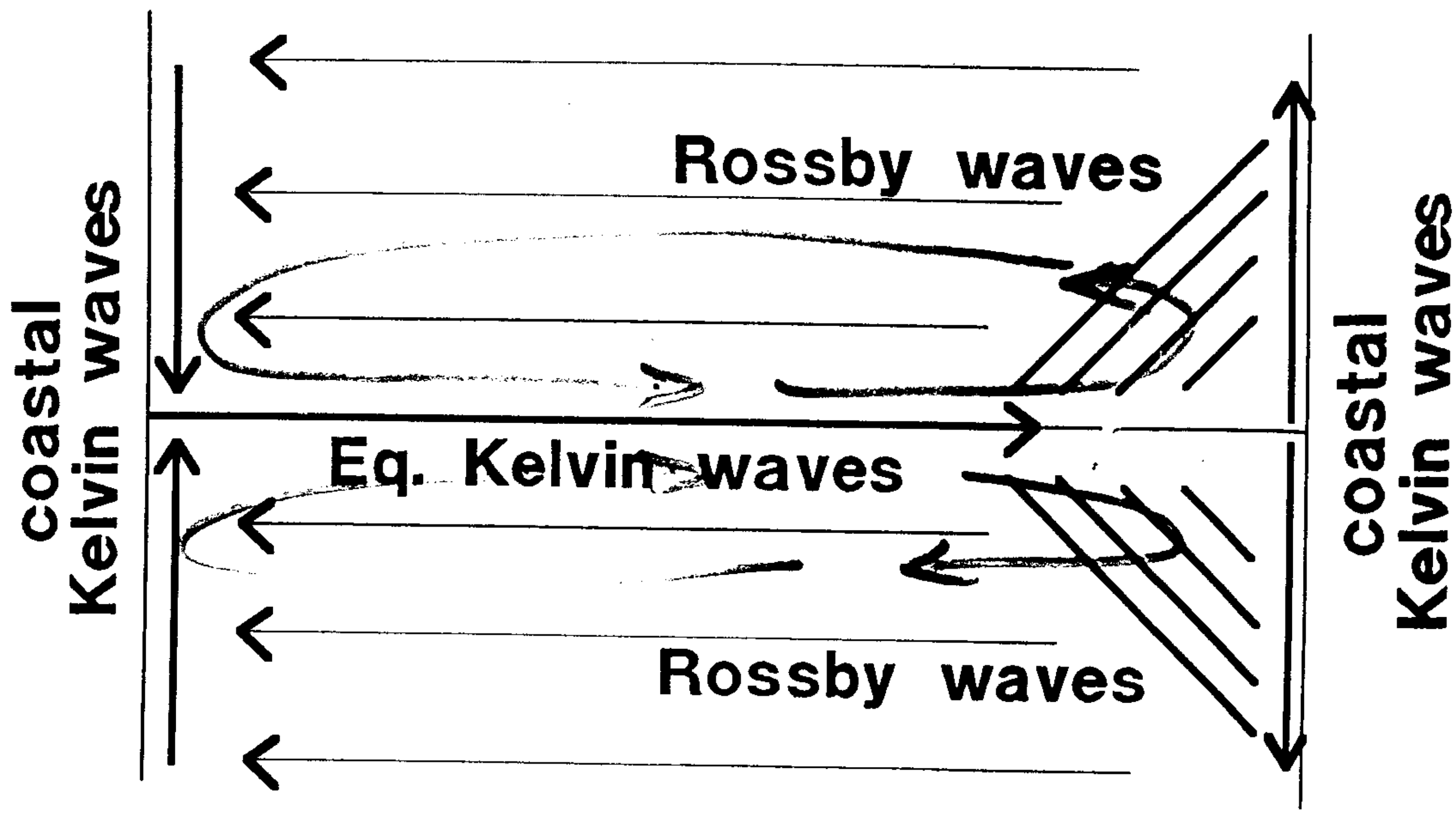
coastal Kelvin waves
Rossby waves
Eq. Kelvin waves
Rossby waves
coastal Kelvin waves

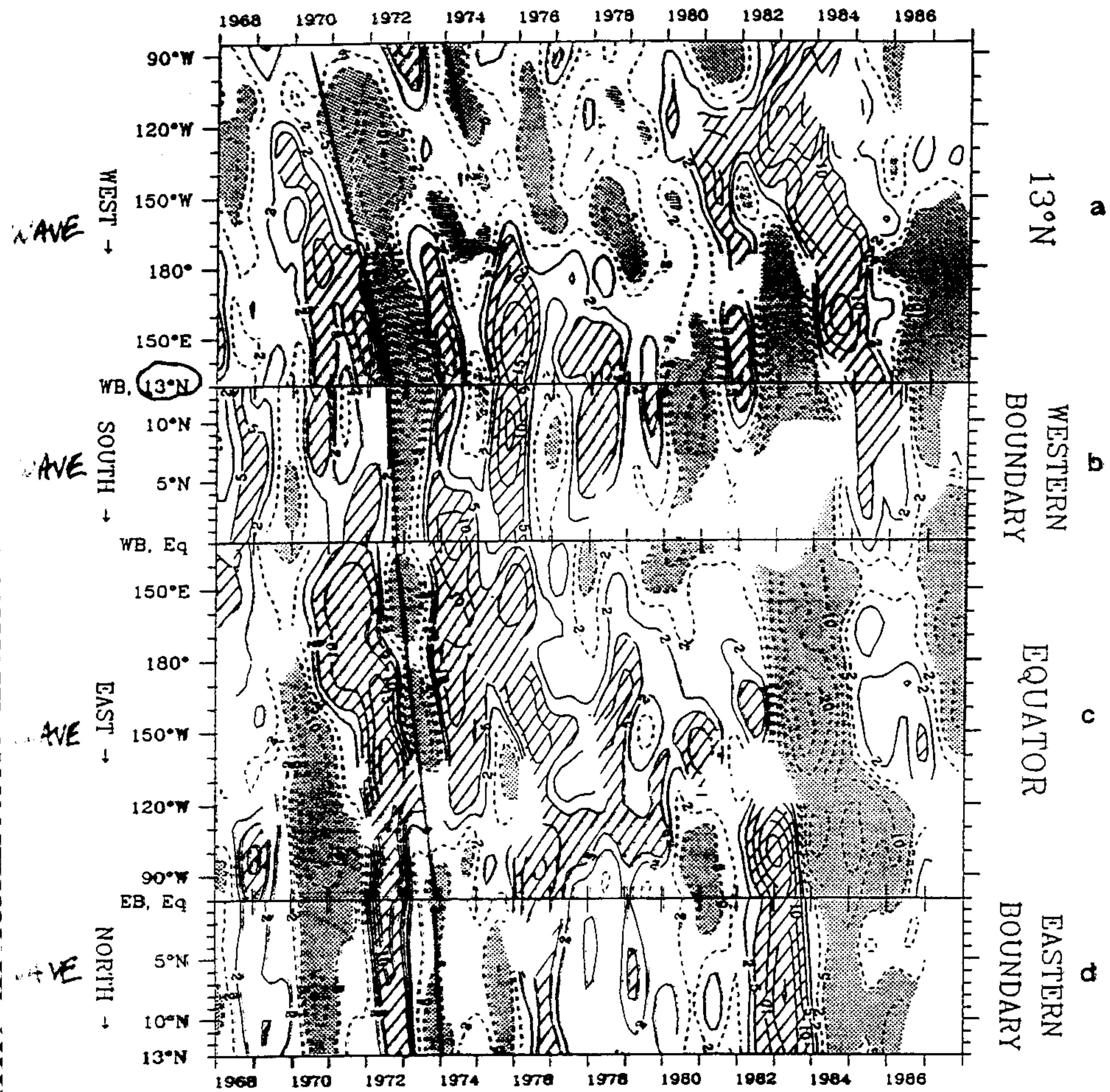

Fig. 24. Time series of anomalous 20°C depth (m) on a circuit around the northern tropical Pacific. (*a*) A zonal section at 13°N, with the eastern boundary at the top. (*b*) A meridional section along the western boundary from 13°N to the equator. (*c*) A zonal section along the equator. (*d*) A meridional section along the eastern boundary, with 13°N at the bottom. The orientation of each section is shown at left. The four sections form a circuit and are continuous at their intersections (including from the bottom edge of the fourth to the top edge of the first). Solid (dashed) contours indicate deep (shallow) anomalies with hatching (stippling) for anomalies greater than 5 m.

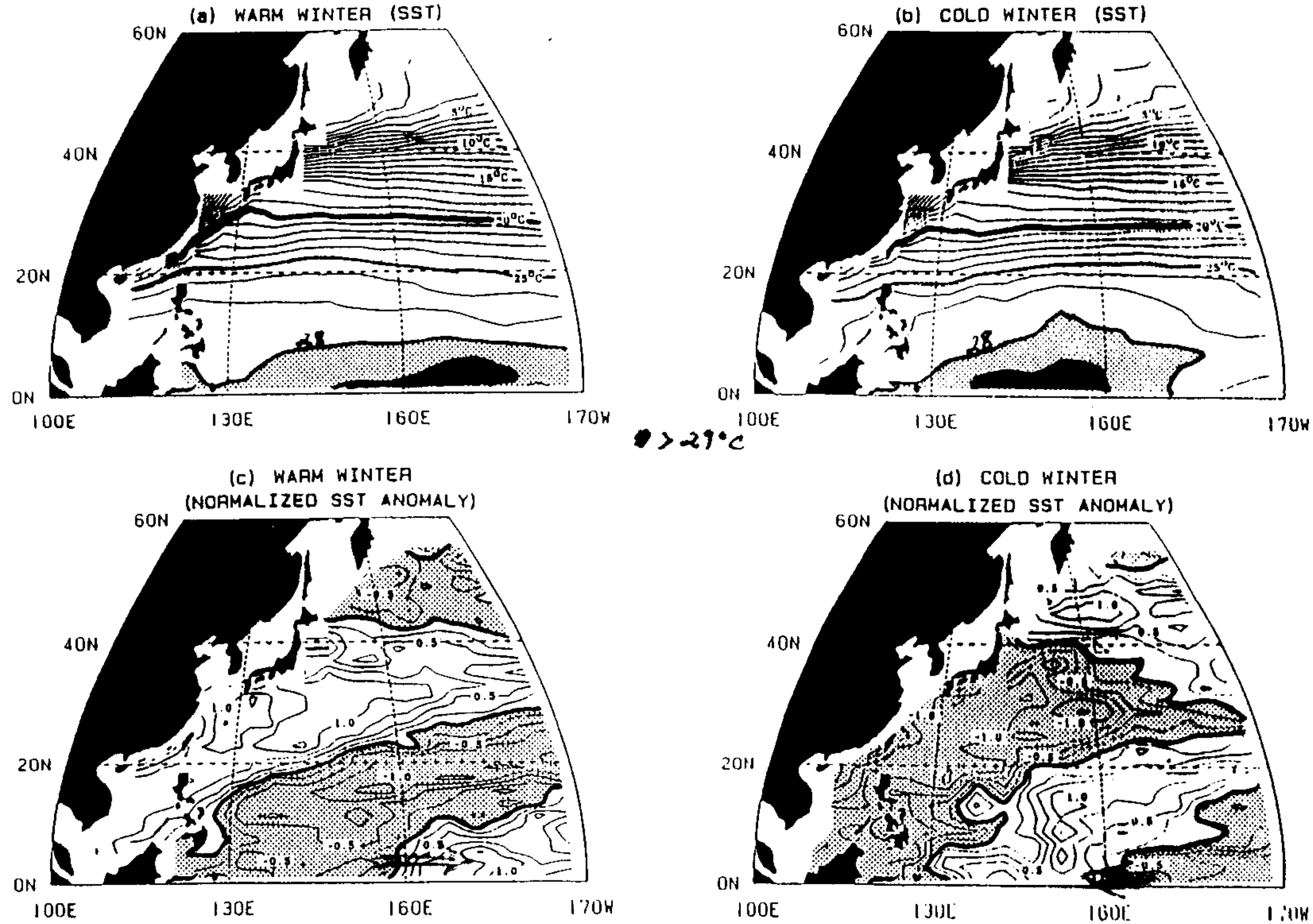

Fig. 3. Composite maps for SST fields for warm (a) and cold (b) winters, and their anomaly fields normalized by the standard deviation at each grid point for warm (c) and cold (d) winters. Contour intervals are 1°C in (a) and (b) and 0.25 in (c) and (d). The dotted areas denote the regions with SST higher than 28°C in (a) and (b), and with negative SST anomalies in (c) and (d).

Wind Stress Anomalies

→ Ocn

... mixing
...nced E
...malous
...thward
Ekman transports

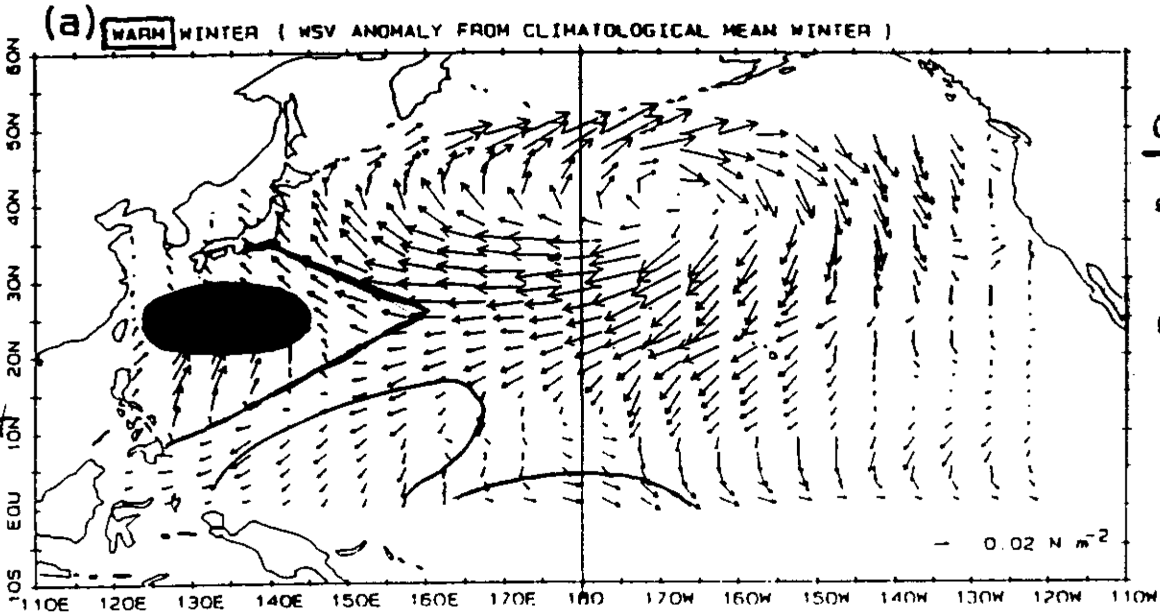

Ocn → Atm

anomalous convergence

westward penetration of trades

...nhanced mixing
...nhanced E
...thward Ekman transport

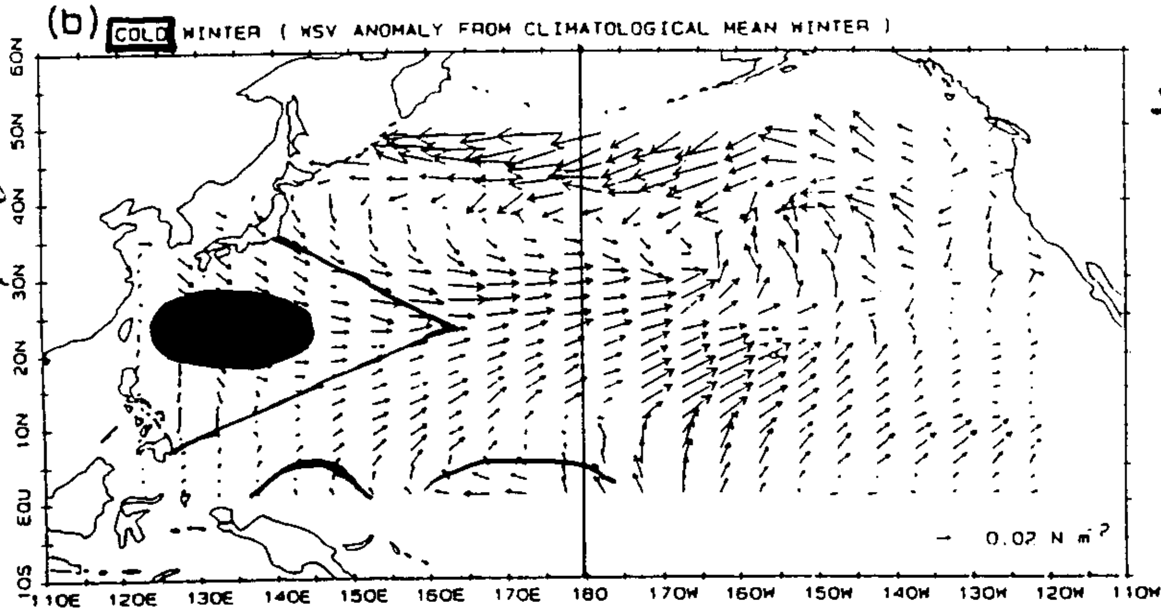

Southward penetration of monsoon westerlies

divergent flow

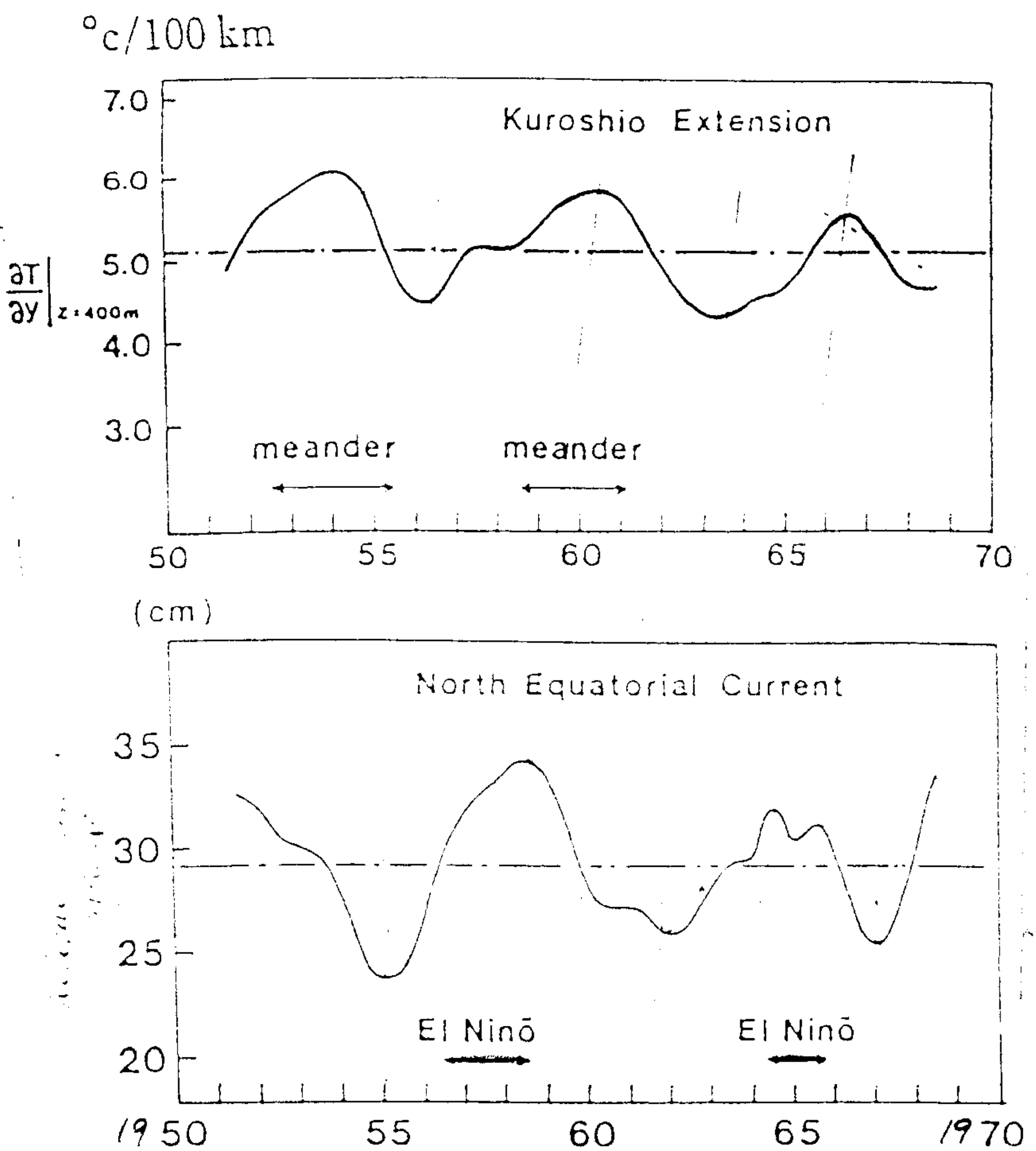

Fig. 8. Two time series of the Kuroshio Extension and the North Equatorial Current filtered using a three-year running mean.

From Yamagata et al. (1985)

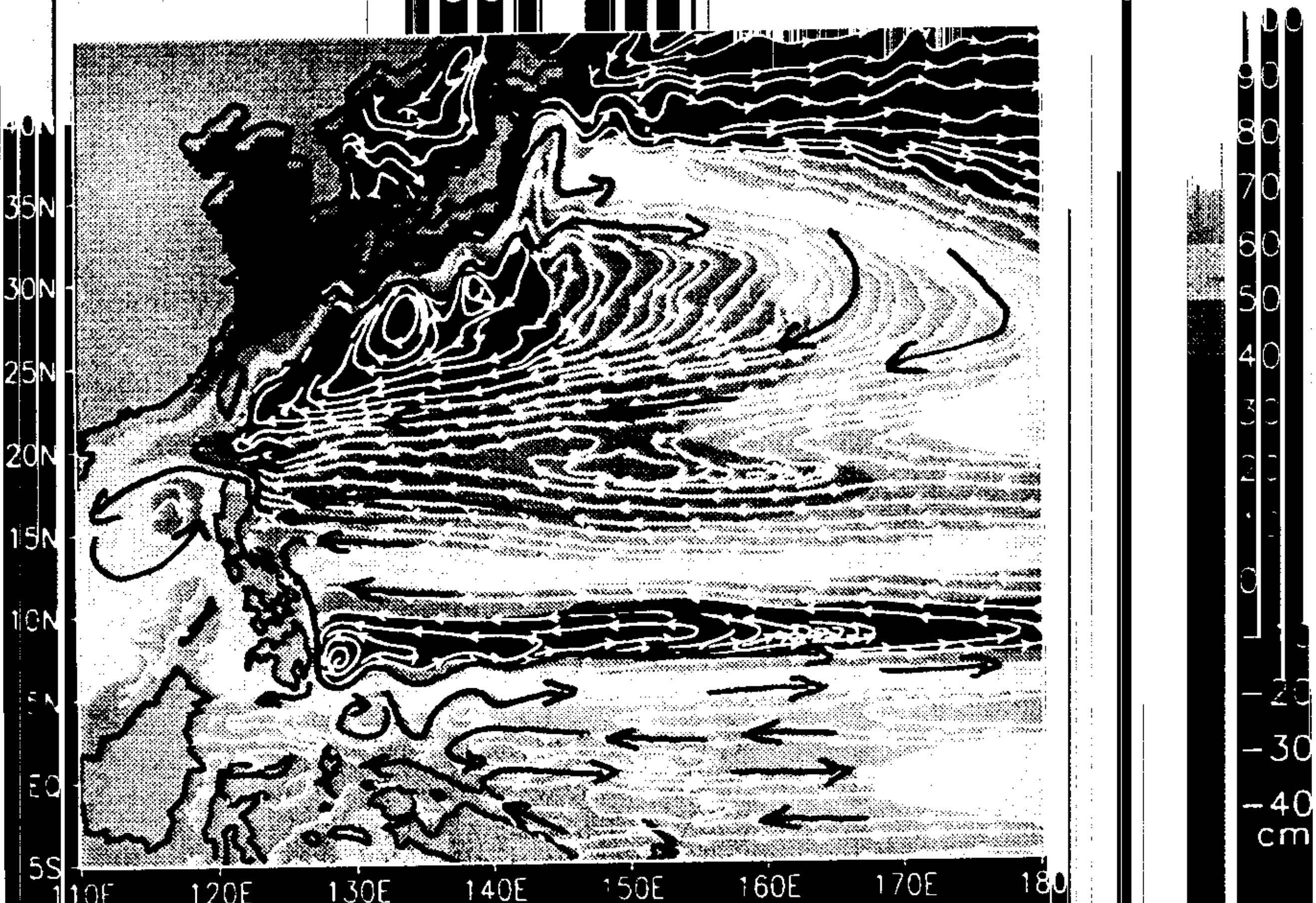

1.5 Layer Model Transports

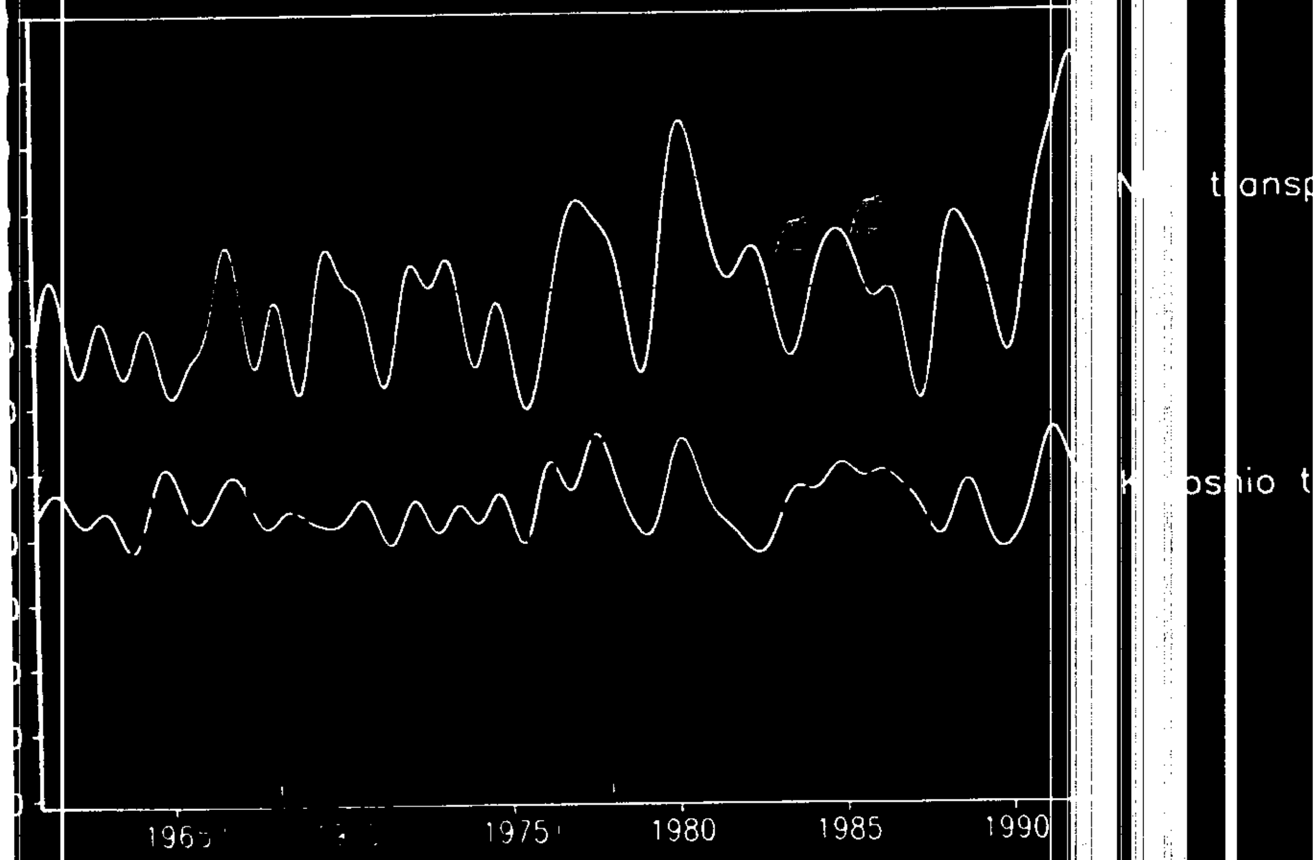

Qiu and Lukas (1995)

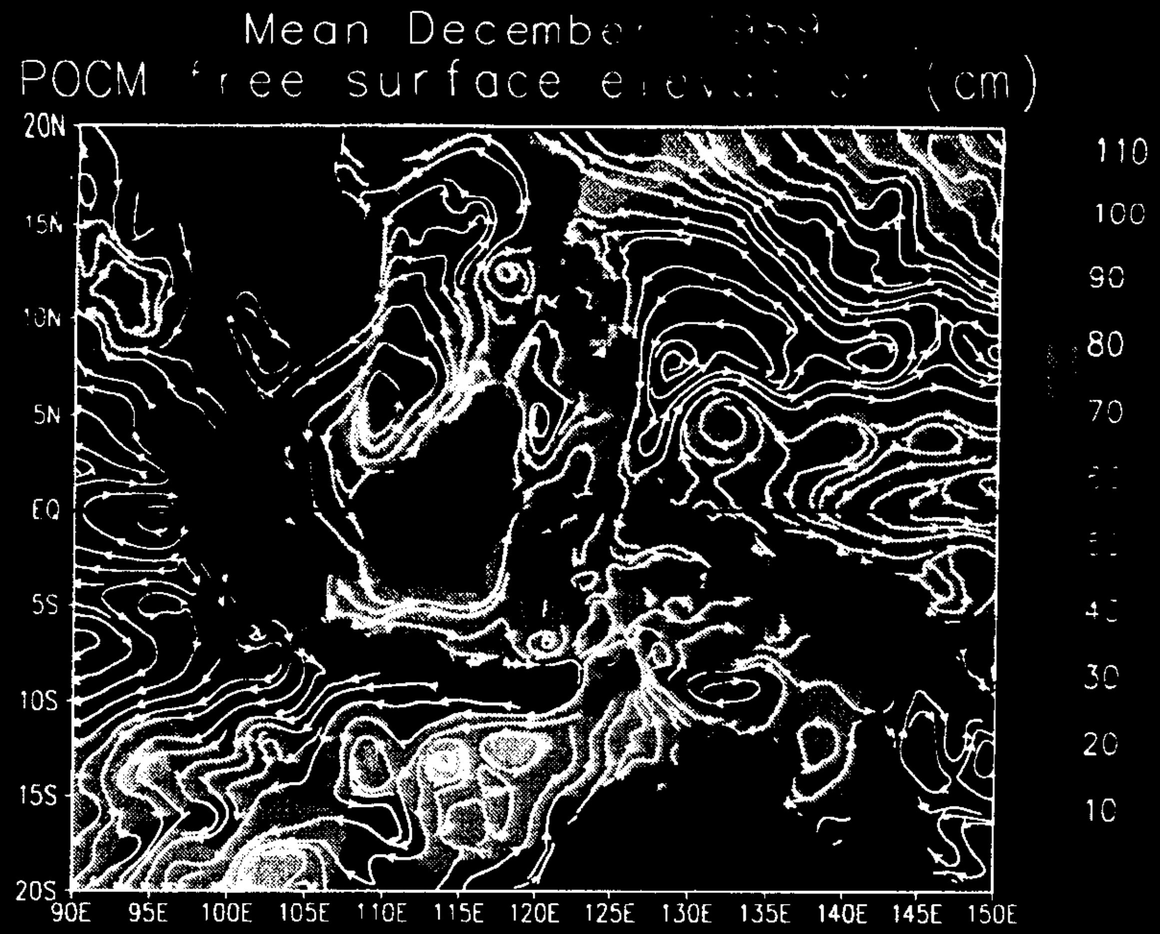
Mean Decembe
POCM
surface
(cm)
20N
15N
5N
EQ
5S
10S
15S
20S
90E
95E
100E
105E
110E
115E
120E
125E
130E
135E
140E
145E
150E
110
100
90
80
70
30
20
10

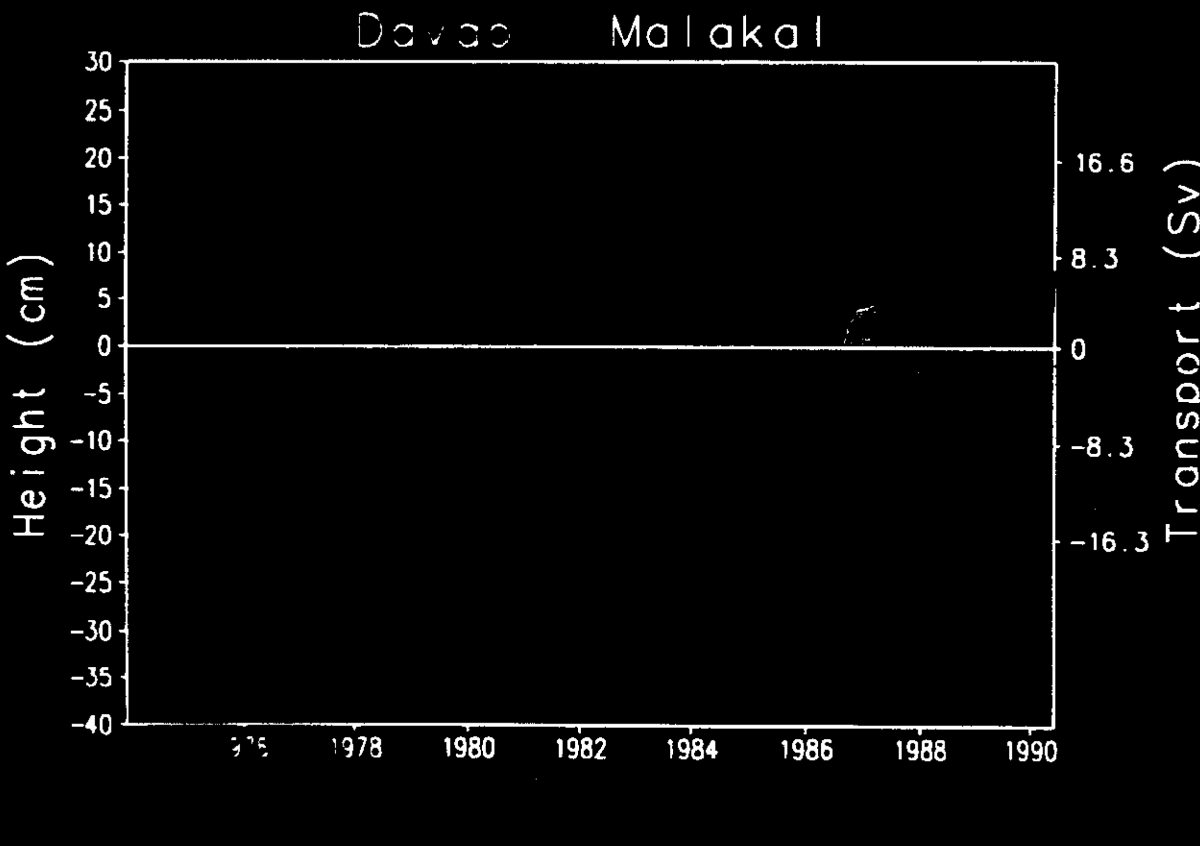
Malakal
Height (cm)
Transport (Sv)
30
25
20
15
10
5
0
-5
-10
-15
-20
-25
-30
-35
-40
16.6
8.3
0
-8.3
-16.3
1978
1980
1982
1984
1986
1988
1990

Indonesia

MEAN CURRENT
LAYER = 1

CLIMATOLOGY DAY 000 TO 365

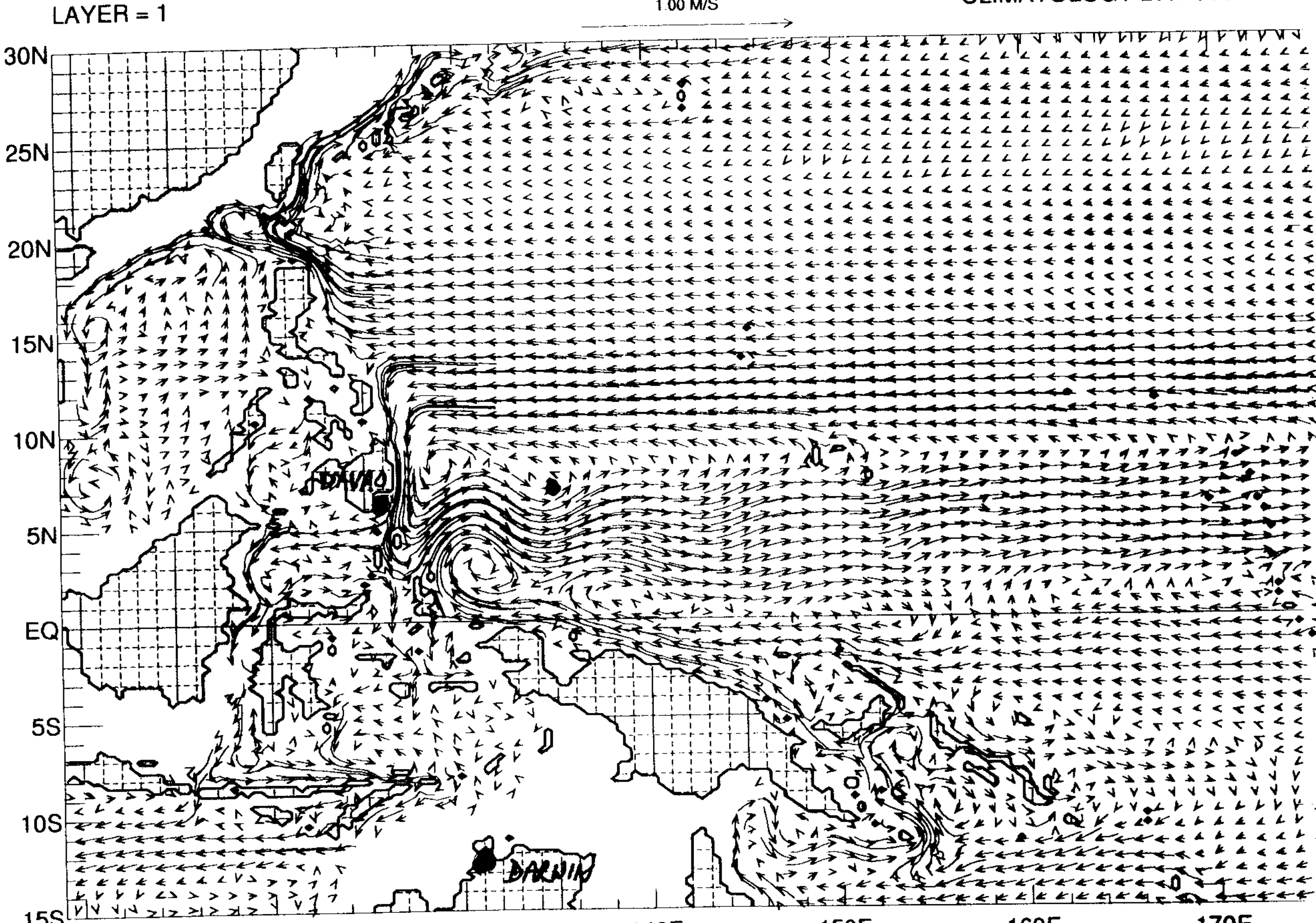

MAX SPEED = 1.797 M/S

W.R.T. 1981-1990 ANNUAL MEAN

J. Kindle (NRL)

NRL 7323 6-Jancourtesy J. Kindle (NOARL)

Anomalous Mindanao Current

TRANSPORT PROFILES

WOM - 115   11521:1: 14.8

P65   (126.00E, 6.50N) TO (128.11E, 6.50N)

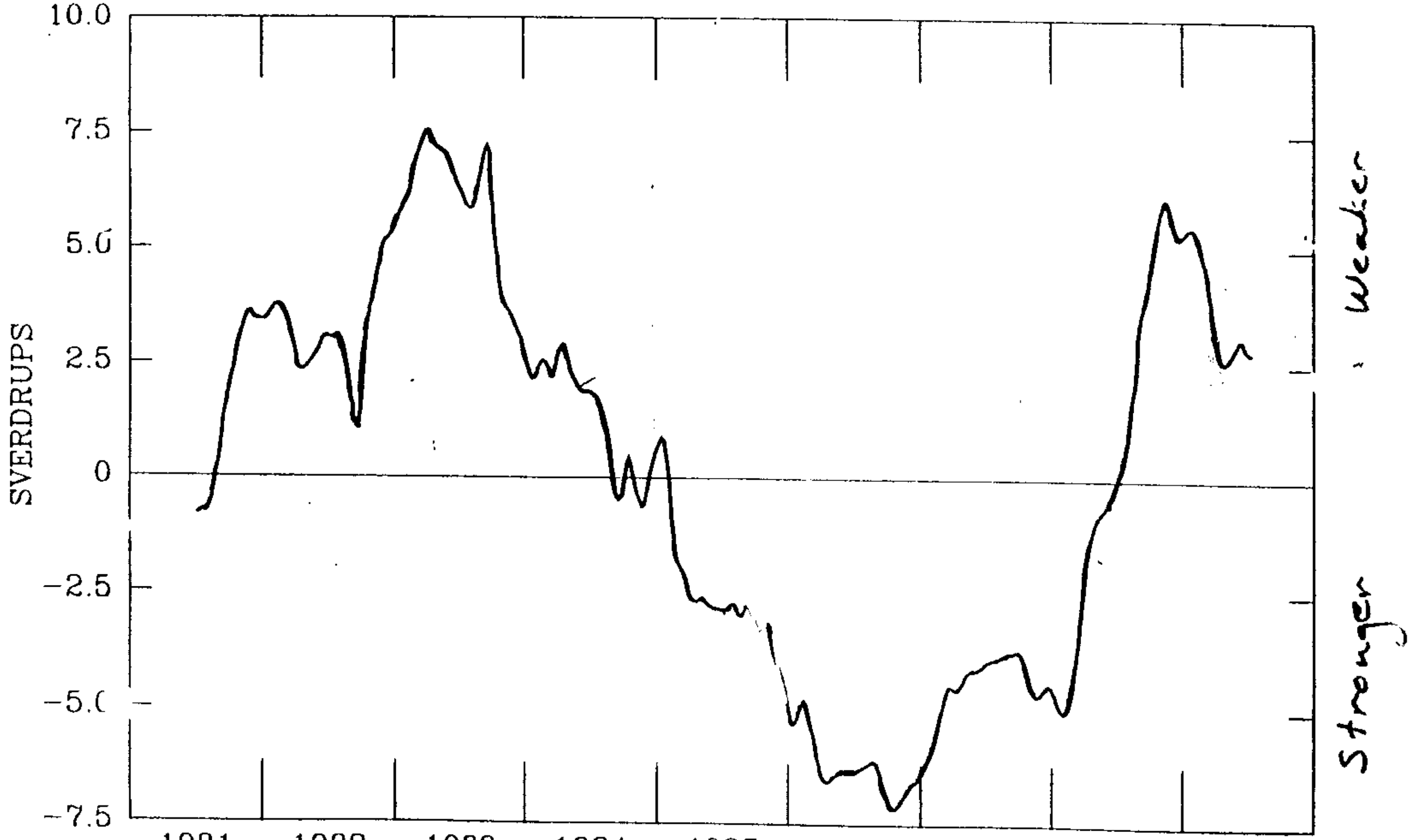

ANOMALIES WRT 81-89 CLIM MEAN (SM364)

NORDA 323 20-FEB-91

Asian-Australian Monsoon system and ENSO

- Competition between land surface processes & ocean-atmosphere interaction
- Extratropical influences on W. Pacific warm pool related to the monsoons

Feedbacks of ENSO on land-locked convection

- Maritime Continent convection strongly affected by ENSO
  - How does this affect the evolution of ENSO?
  - How does this affect the recovery phase?
  - Is this related to eastward migration of warm pool & oceanic convection?
- Impact on monsoonal heat sources
  - dynamic interaction
  - suppression of weaker convection by subsidence from strong source?

Interaction of Asian-Australian Monsoon with ENSO

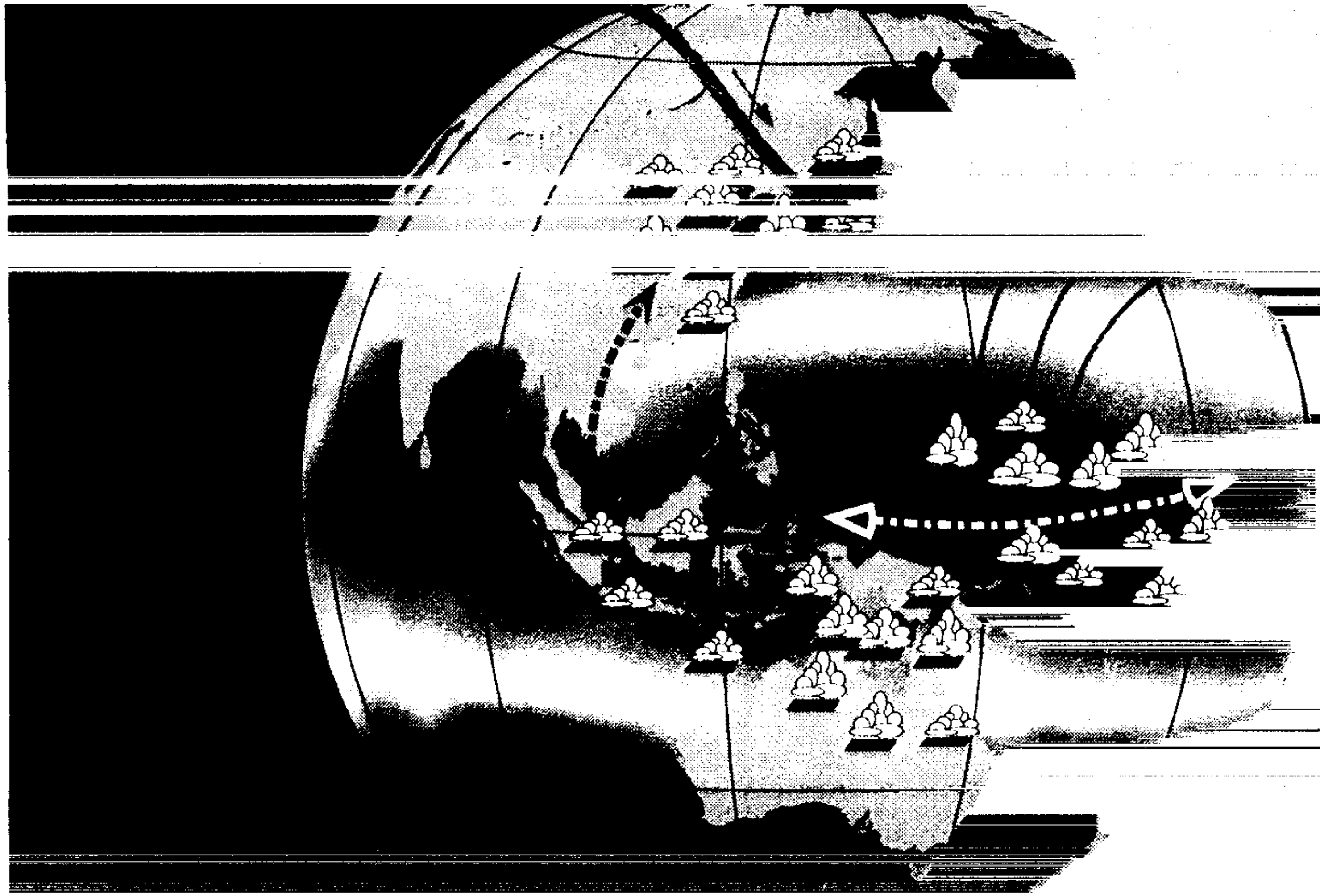

Monsoon feedbacks onto ENSO

- Interannual modulation of the annual Rossby wave
  - can influence warm pool via western boundary reflection and coastal/equatorial Kelvin wave generation
  - can feed back onto subsequent monsoon through meridional advection of SST gradient in W. Pacific
- Asian winter monsoon
  - eastward penetration into W. Pacific depends on warm pool location
- Indonesian throughflow related to strength of monsoon and ENSO

The Low-Latitude Western Boundary Currents in the Pacific and Around Indonesia and their Relationship to ENSO

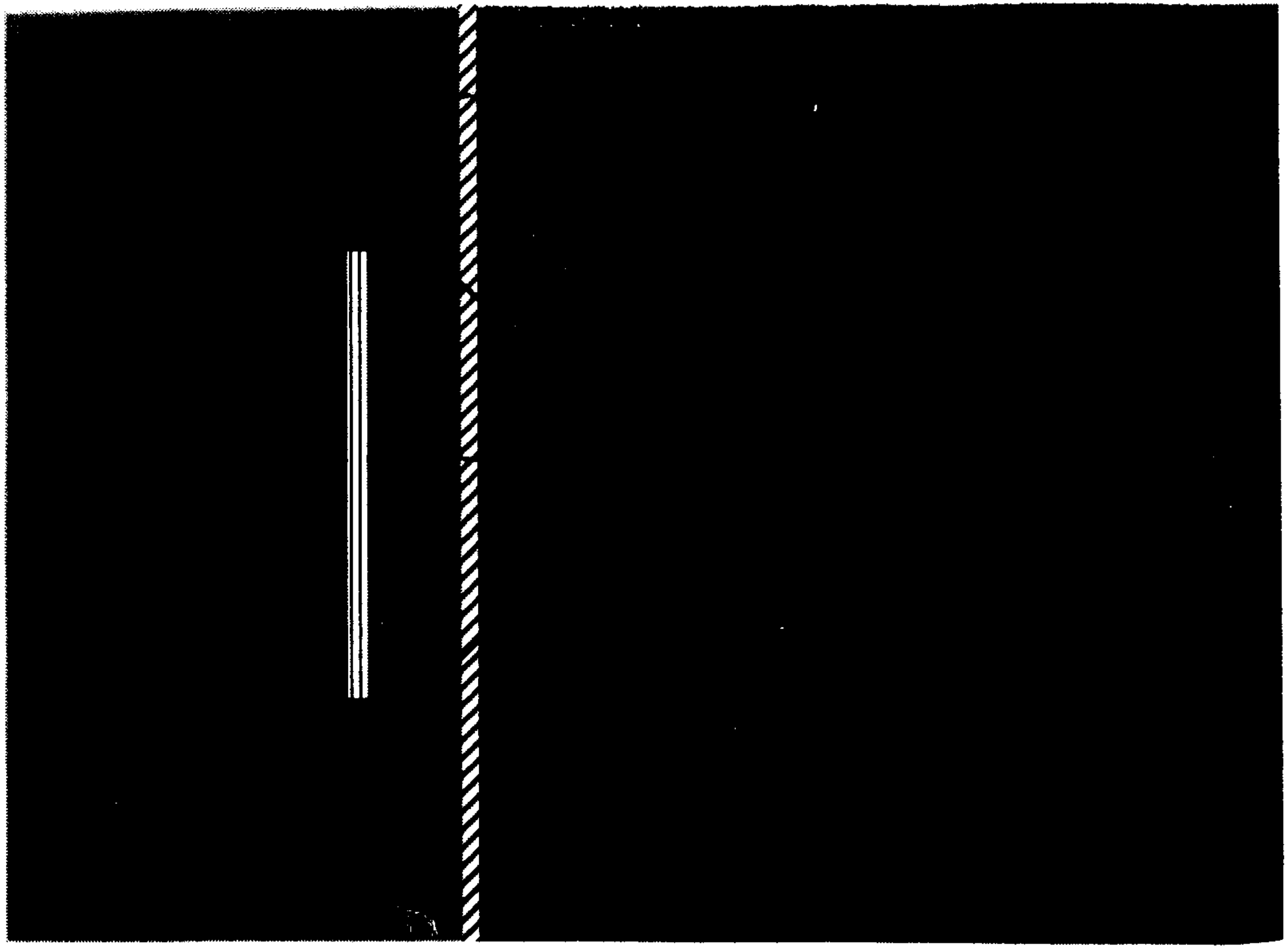

References Related to Monsoon–ENSO Interactions

Barnett, T.P., 1983: Interaction of the monsoon and Pacific trade wind system at interannual time scales. Part I: The equatorial zone. Mon. Wea. Rev., 111, 756-773.

Barnett, T.P., 1991: The interaction of multiple time scales in the tropical climate system. J. Clim., 4, 269-285.

Battisti, D.S. and A.C. Hirst, 1989: Interannual variability in the tropical atmosphere/ocean system: Influence of the basic state and ocean geometry. J. Atmos. Sci., 46, 1687–1712.

Chervin, R.M. and L.M. Druyan, 1984: The influence of ocean surface temperature gradient and continentality on the Walker circulation. Part I: Prescribed tropical changes. Mon. Wea. Rev., 112, 1510-1523.

Cornejo-Garrido, A.G. and P.H. Stone, 1977: On the heat balance of the Walker circulation. J. Atm. Sci., 34, 1155-1162.

Anderson, D.L.T. and J.P. McCreary, 1985a: Slowly propagating disturbances in a coupled ocean-atmosphere model. J. Atmos. Sci., 42, 615-629.

Anderson, D.L.T. and J.P. McCreary, 1985b: On the role of the Indian Ocean in a coupled ocean-atmosphere model of El Nino and the Southern Oscillation. J. Atmos. Sci., 42, 2439-2442.

Chelton, D.B. and M.G. Schlax, 1996: Global observations of oceanic Rossby waves. Science, 272, 234-238.

Hanawa, K., T. Watanabe, N. Iwasaka, T. Suga, and Y. Toba, 1988: Surface thermal conditions in the western North Pacific during the ENSO events. J. Met. Soc. Japan, 66, 445-456.

Hirst, A.C., 1986: Unstable and damped equatorial modes in simple coupled ocean-atmosphere models. J. Atmos. Sci., 43, 606-630.

Hirst, A.C., 1988: Slow instabilities in tropical ocean basin-global atmosphere models. J. Atmos. Sci., 45, 830-852.

Hirst, A.C. and K.-M. Lau, 1990: Intraseasonal and interannual oscillations in coupled ocean-atmosphere models. J. Clim., 3, 713-725.

Jin, F.-F., 1996: An equatorial ocean recharge paradigm for ENSO. J. Atmos. Sci., submitted.

Jin, F.-F., J.D. Neelin and M. Ghil, 1996: El Nino/Southern Oscillation and the annual cycle: Subharmonic frequency-locking and aperiodicity. Physica D, submitted.

Joseph, P.V., J.K. Eischeid, and R.J. Pyle, 1994: Interannual variability of the onset of the Indian summer monsoon and its association with atmospheric features, El Nino, and sea surface temperature anomalies. J. Climate, 7, 81-105.

Ju, J. and J. Slingo, 1996: The Asian summer monsoon and ENSO. Quart. J. Roy. Met. Soc., in press.

Lukas, R., 1988: Interannual fluctuations of the Mindanao Current inferred from sea level. J. Geophys. Res., 93, 6744-6748.

Masumoto, Y. and T. Yamagata, 1990: The birth and evolution of an eastward propagating air-sea coupled disturbance in an aqua-planet. Meteorol. Atmos. Phys., 44, 1-9.

Masumoto, Y. and T. Yamagata, 1991: The response of the western tropical Pacific to the Asian winter monsoon: The generation of the Mindanao Dome. J. Phys. Oceanogr., 21, 1386-1398.

Mitchum, G. and R. Lukas, 1990: Westward propagation of annual sea level and wind signals in the western Pacific Ocean. J. Clim., 3, 1102-1110.

Neelin, J.D., 1991: The slow sea surface temperature mode and the fast-wave limit: analytic theory for tropical interannual oscillations and experiments in a hybrid coupled model. J. Atmos. Sci., 48, 584-606.

Stone, P.H. and R.M. Chervin, 1984: The influence of ocean surface temperature gradient and continentality on the Walker circulation. Part II: Prescribed global changes. Mon. Wea. Rev., 112, 1524-1534.

Webster, P.J. and R. Lukas, 1992: TOGA COARE: The Coupled Ocean-Atmosphere Response Experiment. Bull. Am. Met. Soc., 73, 1377-1416.

Wyrtki, K., 1984: The slope of sea level along the equatora during the 1982/1983 El Nino. J. Geophys. Res., 89, 10,419-10,424.

Wyrtki, K., 1986: Water displacements in the Pacific and genesis of El Nino cycles. J. Geophys. Res., 91, 7129-7132.

Yamagata, T. and Y. Masumoto, 1989: A simple ocean-atmosphere coupled model for the origin of a warm El Nino Southern Oscillation event. Phil. Trans. R. Soc. Lond., 329, 225-236.

Yasunari, T., 1989: A possible link of the QBOs between the stratosphere, troposphere and sea surface temperature in the Tropics. J. Met. Soc. Japan, 67, 483-493.

Yasunari, T., 1990: Impact of Indian Monsoon on the coupled atmosphere/ocean system in the tropical Pacific. Meteor. Atmos. Phys., 44, 29-41.

Zebiak, S.E., 1989: Oceanic heat content variability and El Nino cycles. J. Phys. Oceanogr., 19, 475-486.

Zebiak, S.E. and M. Cane, 1987: A model El Nino-Southern Oscillation. Mon. Wea. Rev., 115, 2262-2278.